Division of Materials Sciences and Engineering
Office of Basic Energy Sciences
US Department of Energy

1. DOE award # and name of the recipient (Institution)

DE-FG02-06ER46290, The Virginia Polytechnic Institute and State University

2. Project Title and name of the PI

Mesoscale Design of Magnetoelectric Heterostructures and Nanocomposites

Dwight Viehland, Materials Science and Engineering, Virginia Tech
Shashank Priya, Mechanical Engineering, Virginia Tech

3. Date of the report and period covered by the report

December 30, 2019:

4. A brief description of accomplishments. This can be in bullet form or whatever you think is useful and appropriate to indicate the sense of progress. Please limit this section to no more than 5 pages.

4.1 Magnetoelectric response in the laser annealed PZT films on amorphous Metglas foil *(Priya)* – Theoretical models have predicted superior ME coupling of PZT/Metglas bulk composites with 2-2 connectivity .[1,2] Yet studies on PZT films deposited on Metglas remain elusive because of the requirement of high temperature (typically at 600-800°C) annealing of PZT that is detrimental to thermally sensitive Metglas with a crystallization temperature of 510 °C.[3,4,5] We provided breakthrough in developing laser annealing of PZT films that opens the opportunity to demonstrate magntoelectric coupling in thermally-sensitive material based layered hetrostructures. Laser irradiation offers a promising alternative to conventional furnace annealing of piezoelectric films deposited on amorphous Metglas. We found that among the large number of processing variables, laser fluence (energy per unit area) plays an important role in governing the thermal gradient evolution that deeply influences the extent of laser-material interaction and thereby the resultant microstructure and electromechanical properties.

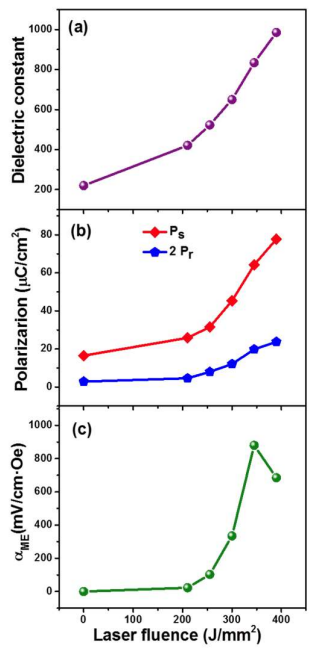

Fig. 1. Variations in values of (a) dielectric constant, (b) saturation (P_s) and remnant (P_r) polarizations, and (c) α_{ME} as a function of laser fluence for PZT/Metglas. Results corresponding to as-deposited condition are represented by the laser fluence of 0 J/mm^2.[6]

A systematic investigation of off-resonance magnetoelectric (ME) response of the $Pb(Zr,Ti)O_3$ (PZT)/ Metglas (FeBSi) bilayered composite by laser annealing was conducted.[6] A continuous-wave 532 nm Nd:YAG laser with varying fluences (210-390 J/mm^2) was utilized to anneal the 2 μm-thick PZT film deposited using granule spray in vacuum (GSV) technique on magnetostrictive amorphous Metglas foil. It was found that the dielectric and ferroelectric properties of the PZT film are strongly affected by the exposed laser fluence, as shown in **Fig. 1**.[6] The ME voltage coefficient (α) of PZT/Metglas increased with the fluence up to 345 J/mm^2, reaching a high value of 880 mV/cm·Oe.[6] The electrical and ME properties were correlated with the changes observed in crystallinity and grain size of the PZT film as well as with the alterations in microstructure and magnetic behavior of Metglas. Our results demonstrated that enhanced ME coupling can be realized in PZT/Metglas film composites by controlling the laser fluence (**Fig. 2**). PZT films of different thicknesses (2-11 μm) were grown on amorphous Metglas foil (25 μm-thick).[7] The variation of theoretical magnitude of αME of the PZT/Metglas as a function of volume fraction of PZT (f_{PZT}) and the interface coupling factor (k) was calculated using the Equation below:[8]

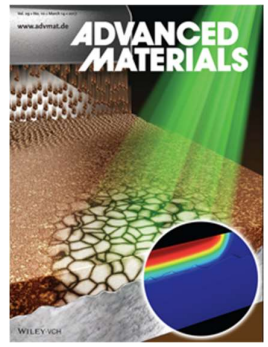

Fig.2 Adv. Mater. 29 (10), 1605688 (2017). Schematic representation of laser annealed RT deposited composite films on Metglas.

$$\alpha_{ME} = \frac{-kf(1-f)(q_{11}^m + q_{12}^m)d_{31}^p}{kv(s_{11}^m + s_{12}^m)\varepsilon_{33}^p + (1-f)(s_{11}^p + s_{12}^p)\varepsilon_{33}^p - 2k(1-f)(d_{31}^p)^2}$$

where the superscripts "p" and "m" represent the piezoelectric and magnetostrictive phases, respectively; k is the interface coupling factor; f denotes the volume fraction of the piezoelectric phase; ε_{33} and d_{31} are dielectric and piezoelectric constants; q_{ij} is piezomagnetic coefficient; and s_{ij}^p s_{ij}^p, and s_{ij}^m s_{ij}^p, and s_{ij}^m and s_{ij}^m are elastic compliances.[8] The theoretical results are plotted in **Fig. 3b**.[7] According to this analysis, the theoretical ME coefficient of the composite with 6 μm-

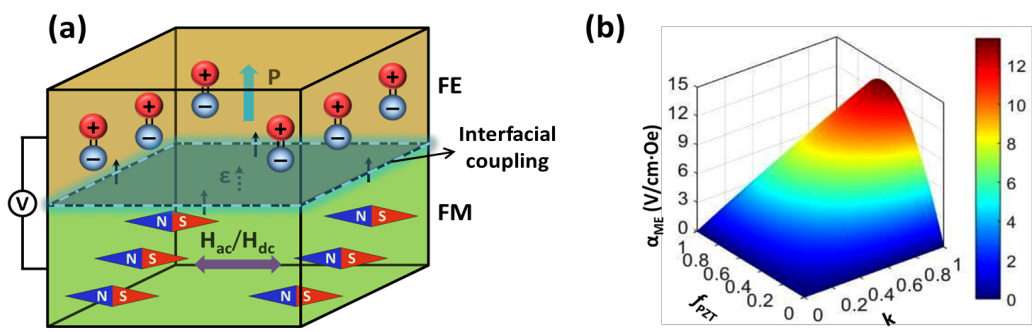

Fig. 3. (a) Schematic representation of the direct magnetoelectric effect in a 2-2 configuration ferroelectric (FE)/ferromagnetic (FM) composite system (the numbers 2-2 refers to the connectivity of the phases in free space). Here the applied magnetic field (H_{ac}/H_{dc}) generates strain (ε) in the magnetic layer via the magnetostriction effect and this strain is transferred to the piezoelectric layer resulting in an electric displacement or dielectric polarization (P) through the piezoelectric effect. (b) Theoretically predicted ME voltage coefficients (α_{ME}) of the PZT/Metglas composite as a function of volume fraction of the PZT (f_{PZT}) layer and the interface coupling factor (k) based on the theory. [7]

thick PZT film and 25 μm m-thick Metglas layer (for fPZT = 0.193 and k = 1) is found to be ~ 7 V/cm•Oe under off-resonance condition.[7] Experimentally we were able to replicate this magnitude of ME coefficient in PZT/Metglas bilayer ME composite.

The improvement in crystallinity of the PZT films by laser annealing is considered to be a major factor in achieving enhanced ME and electrical properties.[5,6] The domain switching increases (quantified by remanant polarization) with the increase in crystallinity of the PZT film, resulting in an enhanced dielectric and electromechanical properties.[9] As the piezoelectric response is directly proportional to the volume of crystalline active phase and reduced clamping, the 11 μm-thick PZT film, if fully annealed, is expected to show better electrical properties than the other lower thickness samples. However, contrary to such expectation, the electrical properties were found to be degraded for thicker (> 6 μm) PZT film. Since all the PZT/Metglas samples with different thickness are fabricated under the same processing conditions, the volume fraction of the annealed PZT phase and its degree of crystallinity are likely to contribute to the thickness dependence of the properties of the PZT/Metglas composites. The sample with 6 μm thick PZT film on Metglas exhibited the largest α_{ME} (7 V/cm·Oe) as predicted by the theoretical calculation (see Fig. 3b). The thickness dependency of α_{ME} was attributed to the differences in the degree of crystallinity and the extent of annealing of the PZT film. The increase in domain switching with increase in crystallized volume of a ferroelectric phase gives rise to enhanced piezoelectricity and improved ME voltage output. A close matching of the measured and calculated α_{ME} values for the 4 and 6 μm thick PZT films on Metglas substrate indicates the optimum fraction of crystallized volume of the PZT phase after laser annealing resulting in adequate combination of mechanical compliance (mechanical impedance matching) and electromechanical properties. The ME output results also suggested that there exists a strong and near-perfect interface bonding ($k \approx 1$), facilitating efficient strain transfer between PZT and Metglas. As expected, the GSV deposited PZT film could withstand thermal stresses caused by laser annealing without exhibiting any delamination from the substrate. Theoretically, the ME voltage coefficient should increase continuously with increase in thickness of the PZT film (grown on 25 μm thick MS substrate) up to 33 μm (volume fraction f_{PZT} = 0.56), but the experimental data did not exhibit such trend. This phenomenon was considered to be related with the extent of laser interaction in thicker PZT films.

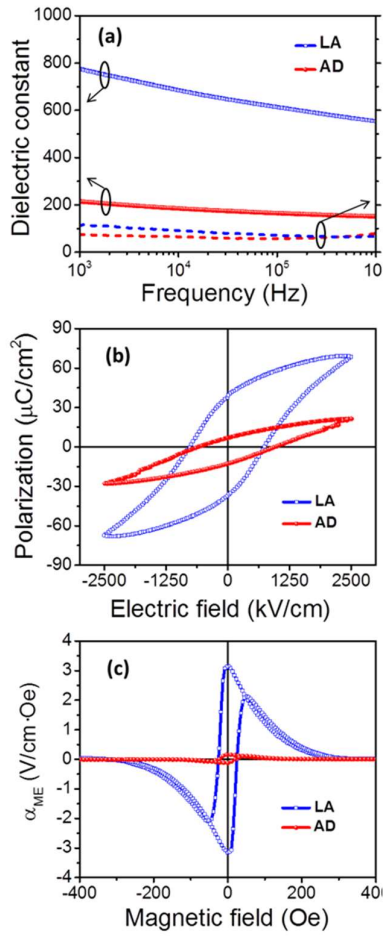

Fig.4. (a) Dielectric properties and (b) Polarization hysteresis loops of the as-deposited and laser annealed PZT

Enhanced self-biased magnetoelectric coupling in laser annealed Pb(Zr,Ti)O_3 thick film deposited on Ni foil: We further demonstrated enhanced and self-biased magnetoelectric coupling in a laminate heterostructure comprising of 4 µm-thick PZT film deposited on 50 µm-thick flexible Nickel (Ni) foil. In this experiment, granule spray in vacuum (GSV) deposited PZT film was annealed using laser radiation at room temperature without interfacial chemical reactions. Laser induced crystallinity improvement in PZT thick film led to enhanced dielectric, ferroelectric and magnetoelectric (>1300% increase) properties of the PZT/Ni composite, as shown in Fig. 4. Self-biased *ME* response on the order of 3.15 V/cm·Oe was obtained from the laser annealed PZT film deposited on Ni (Fig. 4(c)). This is one of the highest reported value among similar ME composite systems. The tunability of self-biased *ME* coupling in PZT/Ni laminate composite has been found to be related to the demagnetization field in Ni, strain mismatch between PZT and Ni, and flexural moment of the composite structure. Phase-field model provided quantitative insight into these factors and illustrated their contribution towards observed self-biased *ME* response.

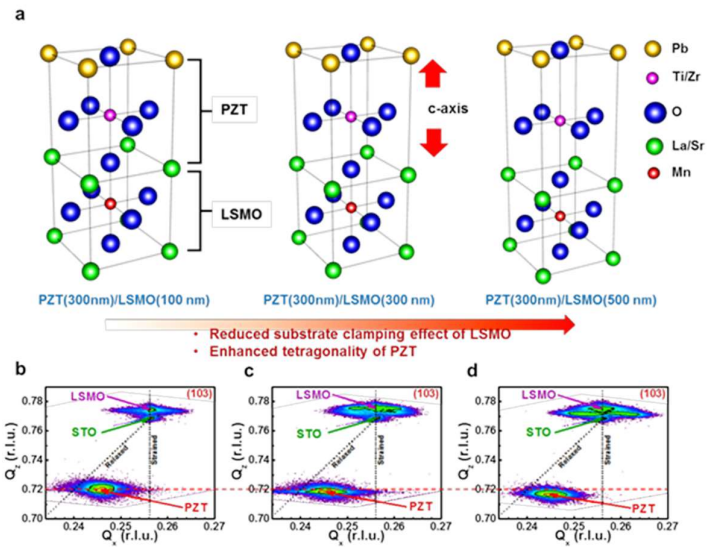

Figure 5. (a) Schematic illustration of the effect of strain engineering on the ME composite crystal structure. (b) RSM of PZT/LSMO 100 nm (c) RSM of PZT/LSMO 300 nm (d) RSM of PZT/LSMO 500 nm.

4.2 Fundamental understanding of magnetodielectric (MD) coupling in PZT/LSMO epitaxial films (Priya)

The lattice misfit strain, along with strong clamping effect from the substrate, degrades both piezomagnetic and piezoelectric coefficients leading to reduced ME coupling in the hetero-epitaxial ME composites. We studied strain-engineered c-axis oriented epitaxial LSMO and PZT thin films, as illustrated in Figure 5. In order to maximize the MD response, we modulated the interface charge state through the ferroelectricity of the PZT layer, which enhanced the room-temperature magnetic properties of LSMO and resulted in a room-temperature MD effect. To confirm the residual strain in the PZT and LSMO films, asymmetric reciprocal space map (RSM) analysis was performed around the (103) reflection (Figure 5 (b)-(d)). The LSMO layer was found to be fully tensile-strained with respect to STO, whereas the PZT layer was found to be under compressive strain. The reciprocal lattice point (RLP) of the PZT layer is shifted towards lower Q_z values with increasing LSMO layer thickness, indicating an increase in the residual compressive strain in the PZT layer. Because of the significant residual strain with respect to the LSMO layer, the PZT layers exhibited partially relaxed RLP

positions. Role of this intrinsic strain in determining the frequency dependent behavior is of significant interest as ME and MD effects are both strain-driven phenomenon.

To evaluate the magnetic characteristics of the LSMO layers, magnetization measurements were performed as a function of temperature and induced DC magnetic field. The Curie temperature (T_C) was shifted towards lower temperatures in the 100 nm-thick LSMO film, which corresponds to the case of the highest tensile strain with respect to the STO substrate. Conversely, the 500 nm-thick LSMO film exhibited a higher degree of strain relaxation and thus a higher T_C. We therefore concluded that tensile strain in epitaxial LSMO films acts to shift the observed T_c towards lower temperatures. [10] The 100 nm-thick LSMO film had a T_c at RT and small magnetization (~52 emu/cm^3). However, the 500 nm-thick LSMO film exhibited substantial magnetization (215 emu/cm^3), resulting in large magnetostriction. However, the magnetic properties of the LSMO films were found to degrade following PZT deposition. This degradation can be attributed to interfacial magnetic reconstruction due to electrostatic charge accumulation at the PZT/LSMO interface by ferroelectric spontaneous polarization.[11,12] The interfacial charge accumulation can modulate the valence state of Mn from high spin state Mn^{3+} to the low spin state Mn^{4+} at the interface and changes the magnetic moment of the LSMO interface.[12] The MD response of the PZT/LSMO composites was found to increase with increasing LSMO layer thickness. Strain engineering via control over the LSMO layer thickness leads to an enhanced magnetic moment at RT via the simultaneous shifting of T_c and a reduction of the substrate clamping effect, thereby providing a 24% MD coefficient at RT. We further investigated the influence of interface charge modulation, via controlling the ferroelectric polarization direction, on the magnetic moment of LSMO in order to enhance the MD response of the PZT/LSMO composites. In order to confirm the initial polarization state of the PZT film, the ferroelectric domain structure and polarization switching behavior of the PZT film were investigated, as shown in Figure 6(a) and (b). The ferroelectric domain clearly show 180° domain motion without pinned domain wall, as shown in Figure 6(b). The polarization direction was determined by the corresponding poling direction. As a result, the initial polarization exhibited the +P state (outer region in Figure 6b), which drove interface charge accumulation.[12,13]

Investigation of the electronic band structure at the PZT/LSMO hetero-interface was performed via X-ray photoelectron spectroscopy (XPS) analysis of the PZT/LSMO epitaxial composite. In order to determine the heterointerface valence band offset, ΔE_V, the following XPS spectra were recorded: (i) the Pb 4f core level (CL) and PZT valence band maximum (VBM) from the thick PZT film; (ii) the La 4d CL and LSMO VBM from the LSMO strain-template; and (iii) the Pb 4f and La 4d CLs from ~2 nm PZT on LSMO, representative of the PZT/LSMO interface. Residual surface contaminants were removed in-situ via a 5 s low-energy Ar^+ ion sputter prior to all XPS measurements. Utilizing the method introduced by Kraut et al., ΔE_V can be determined as follows:[14]

$$\Delta E_V = \left(E_{Pb\,4f}^{PZT} - E_{VBM}^{PZT}\right) - \left(E_{La\,4d}^{LSMO} - E_{VBM}^{LSMO}\right) - \Delta CL(i)$$

where $E_{Pb\,4f}^{PZT}$ and $E_{La\,4d}^{LSMO}$ are the CL binding energies from the thick PZT and LSMO films, respectively, E_{VBM} is the VBM for each material, and $\Delta CL(i)$ is the measured binding energy separation between the Pb 4f and La 4d CLs recorded at the PZT/LSMO interface, i.e., $\left(E_{Pb\,4f}^{PZT} - E_{La\,4d}^{LSMO}\right)$. E_{VBM} was determined by performing a linear regression fitting of the

measured intensity at the onset of photoemission with respect to the background-dependent spectral baseline.[15] The conduction band offset, ΔE_C, can then be calculated using:[15]

$$\Delta E_C = E_g^{LSMO} - E_g^{PZT} - \Delta E_V$$

where E_g^{PZT} and E_g^{LSMO} are the band-gap energies of PZT and LSMO, respectively. Figure 6c shows the measured CL and valence band (VB) spectra taken from the thick PZT, thick LSMO, and thin PZT on LSMO films, respectively. The measured BE separations were found to be 136.56 eV, 100.86 eV, and 36.45 eV for the $\left(E_{Pb\,4f}^{PZT} - E_{VBM}^{PZT}\right)$, $\left(E_{La\,4d}^{LSMO} - E_{VBM}^{LSMO}\right)$, and $\left(E_{Pb\,4f}^{PZT} - E_{La\,4d}^{LSMO}\right)$ separations, respectively. The resulting ΔE_V was found to be 0.75 ± 0.05 eV. Similarly, ΔE_C was calculated to be 1.85 ± 0.1 eV, as determined using the measured ΔE_V, band-gap energies of 3.6 eV and 1.0 eV for PZT and LSMO, respectively. We assume band-gap energies for PZT and LSMO of 3.6 eV and 1 eV, respectively, as shown in the band diagrams of the PZT/LSMO hetero-interface in the +P polarization state.[16] The internal electric field within the interface depletion region may produce a potential drop across the depletion region (having thickness *d*), shifting the relative positions of the valence and conduction bands of LSMO outside of the depletion region (Figure 6d). Electron and hole accumulation at the interface, with respect to the polarization direction of the PZT layer, results in band bending in the LSMO electrode layer. Since the initial polarization in the PZT layer is aligned with the +P state, we expect that the interface maintains an accumulation state, which degrades the interface magnetic moment of the LSMO layer (Figure 6e). This may depress the magnetostriction between the PZT/LSMO layer as a result of strain propagation across the interface. Therefore, in order to achieve strong ME coupling in PZT/LSMO heterostructures, a charge depletion state should be induced at the PZT/LSMO interface. Optimized films with strain engineered configuration provided a large magnitude of MD coefficient.

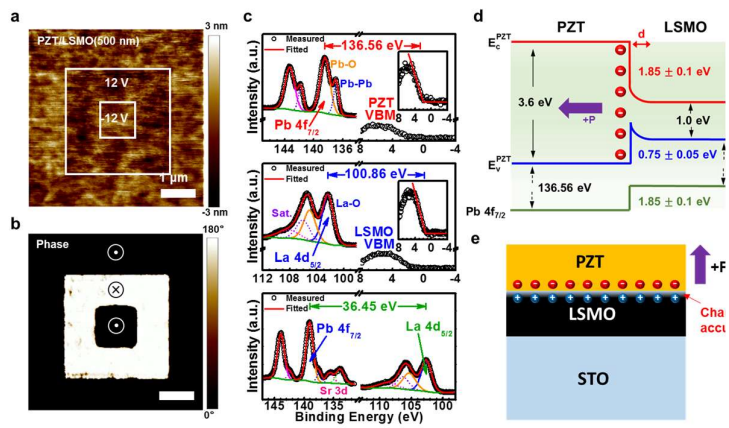

Figure 6. (a) Surface AFM image of PL5 with marked polarization switching voltage condition. DC biases of 12 V and -12 V were applied on a 3 × 3 μm^2 area and 1 × 1 μm^2 area. (b) Piezoelectric response phase image. Arrows indicate polarization direction. (c) XPS spectra of the PZT and LSMO layers used in the calculation of the interfacial energy band discontinuities (d) Energy band diagram of the PZT/LSMO hetero-interface in the initial accumulation state. (e) Schematic of charge accumulation in the initial PZT/LSMO hetero-epitaxial film.

4.3 BiFeO$_3$ on Piezoelectric PMN-PT (Viehland)

• ***Growth and Deposition Studies.***

One of the goals of this program was to induce the cycloidal to antiferromagnetic phase transition in BiFeO$_3$ (BFO) by epitaxial strain and external applied electric field (E). High-

quality epitaxial BFO thin films were successfully deposited on $Pb(Mg_{1/3}Nb_{2/3})O_3$-30at%$PbTiO_3$ (PMN-30%PT) substrates by pulsed laser deposition (PLD). The effects of film thickness, laser energy density, and PMN-30PT substrate orientation on BFO epitaxial thin layers were systematically studied.

Growth of $BiFeO_3$ on Piezoelectric PMN-PT: To optimize the deposition conditions, firstly BFO layers were deposited on $SrTiO_3$ (STO) and $LaAlO_3$ (LAO) substrates. Deposition conditions such as target-substrate distance, substrate temperature, oxygen partial pressure, pulse rate, annealing time, atmosphere, and etc., were studied by a series of experiments. Thin film x-ray diffraction (XRD), atomic force microscopy (AFM), and scanning electron microscopy (SEM) were employed to determine the crystal structure, surface morphology and film thickness, respectively. A $SrRuO_3$ (SRO) buffer layer was deposited between the BFO layer and the substrate, as an electrode by which to apply E onto the substrate. Even though SRO is not piezoelectric, this allowed us to optimize its deposition conditions.

Next, efforts were placed upon improving the techniques for obtaining smooth and polished PMN-PT substrates. A three-step polishing method was developed by which to obtain relatively smoother PMN-PT substrates with surface roughness less than 3nm (see Figs. 7a-c). To verify the substrates ferroelectric/piezoelectric transformation (or Curie) temperatures, temperature dependent dielectric constant measurements were performed, which was done before polishing so that the Au electrodes would be removed. This enabled us to know the substrate composition fairly accurately, as PMN-PT is a solid solution.

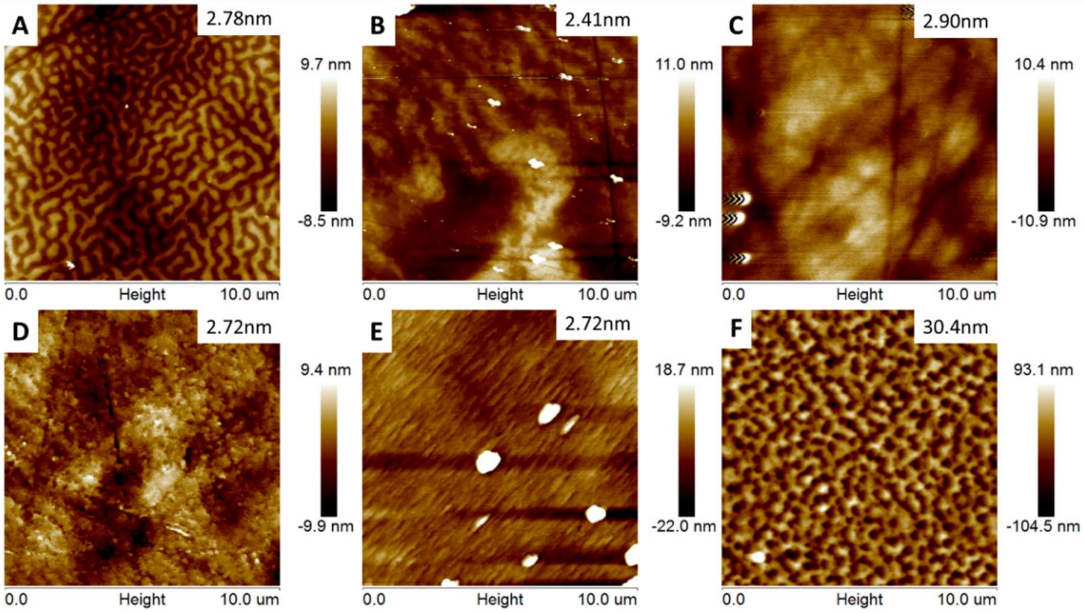

Figure 7. AFM images of (a)-(c) polished PMN30PT, and (D)-(F) BFO(50nm)/SRO(5nm)/ PMN30PT. The orientations of PMN-PT are (a)(d) (100), (B)(E) (110), and (C)(F) (111). The surface roughness is given in the inset.

After these prerequisite investigations, epitaxial BFO/SRO heterostructure layers were deposited on PMN-30PT. In order to tune the epitaxial strain of BFO, the effects of film thickness, laser energy density, and PMN-PT orientation were studied. Finally, an E-field was applied to the PMN-PT to change its lattice parameters via piezoelectricity, and the strain changes transferred to the BFO heterostructural layer were measured by XRD.

Thickness and Laser Energy Density Effects on BFO: Figures 8a and 8c show the effect of BFO and SRO layer thickness on the epitaxial strain of BFO. Although the laser energy densities are different (~3J/cm^2 in 2A and ~1J/cm^2 in 2C), the thickness effects exhibit the same trend. With increase of layer thickness for either the SRO (5nm to 20nm) or BFO (50nm to 100nm), the BFO peaks were shifted to lower 2θ values, indicating that the in-plane tensile strain of BFO decreases. The reason is that thicker SRO or BFO layers relax the strain of BFO.

Figure 8b shows the effect of laser energy density. As the energy density was reduced from 3J/cm^2 to 1.5J/cm^2, the strain of the BFO layer was fairly constant. However, on decreasing the energy density to below 1.15 J/cm^2, the tensile strain of the BFO layer was significantly increased to about 0.45%. Slower growth rates may allow for better epitaxy, and improve the quality of the BFO layer to some extent. According to Figs. 8a-c, BFO(50nm)/SRO(5nm) heterostructure layers deposited using a 1.00J/cm^2 laser energy density had the largest in-plane tensile strain.

Figure 8d shows the changes along the out-of-plane direction of the BFO(50nm)/SRO(5nm) heterostructure under application of E to (100) PMN-30PT. In order to calculate the in-plain strains, Gaussian fits were used to obtain the precise positions of the BFO peaks. Upon increasing the field from 0<E<9kV/cm, the in-plane strain of BFO changed from 0.45% to 0.37%. Following the previously predicted epitaxial phase diagram of the spin states of BFO [1], this is close to the boundary between type-II cycloid and homogeneous antiferromagnetic states (□≈0.5%), as can be seen in Figure 9.

The E-induced changes to the in-plane strains of other heterostructure layers, such as BFO(70nm)/SRO(5nm) (Fig 8e) and BFO(50nm)/ SRO(10nm), were also measured (see Fig. 8f). The values of the BFO layer's in-plane strains were changed with increasing E up to 10kV/cm from 0.169% to 0.105%, and from tensile 0.076% to compressive -0.043%, respectively. Again, following the predicted epitaxial phase diagram of the spin states of BFO, the latter exactly changes across the boundary between type-I and type-II cycloid states (0%).

Accordingly, by tuning the thicknesses of the BFO and SRO layers, the in-plane strain of BFO was varied due to stress relaxation. By applying an out-of-plane E field modulation, the value of these in-plane strains were tuned across the predicted different magnetic phase boundaries. Hopefully, in the near future, we realize the E-induced cycloidal-

antiferromagnetic phase transition of BFO, releasing the magnetoelectric interactions of BFO that are trapped within the spin cycloid.

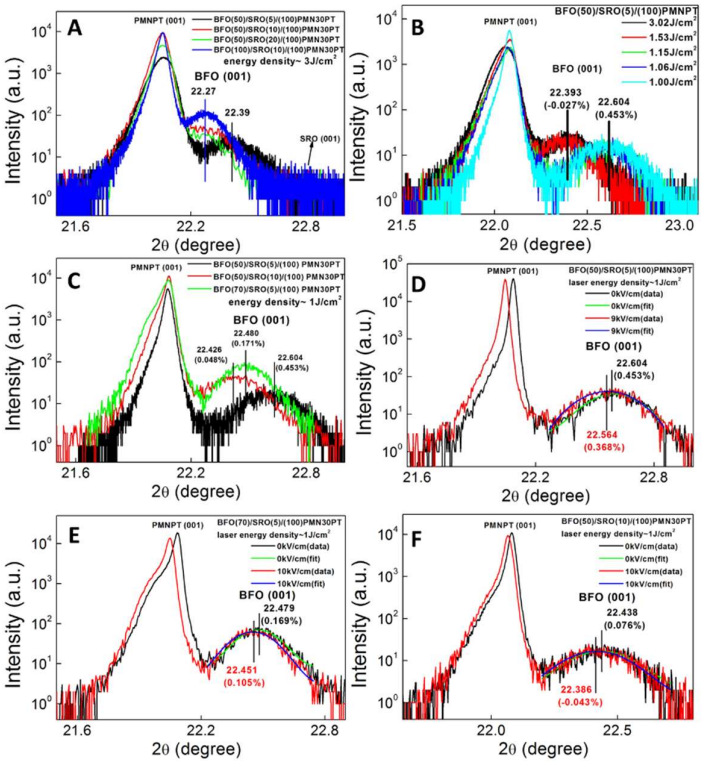

Figure 8. Thin film XRD patterns of BFO/SRO/(100) PMN30PT. (a),(c) thickness effects. (b) Laser energy density changed from 3.02 to 1.00J/cm^2. (d)-(f) BFO samples with different thicknesses under E=0 and 10kV/cm, where the in-plane strains are given inside the brackets.

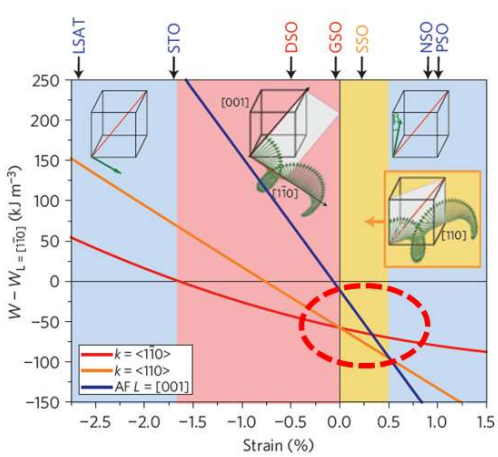

Figure 9. Magnetic phase diagram of strained BFO films. The stability of the different states are shown in colours (blue: homogeneous antiferromagnetic; red: type I cycloid; orange: type II cycloid). The different substrates used are located at the top of the diagram at their corresponding strain. [1] D. Sando, et al., Nature Materials 12, 641 DOI:10.1038/NMAT3629 (2013).

<u>*PMN-PT Orientation Effects on BFO :*</u> (110) and (111) PMN-30PT were then chosen as substrates upon which to deposit BFO(50nm)/SRO(5nm) heterostructure layers, with the goal of determining the orientation effects on BFO's strain. The layer deposition conditions were adjusted in a similar manner as for those grown on (100) PMN-PT, given above. The BFO layers on (110) PMN-30PT had similar surface roughness (see Fig. 7e) as

that grown on (100) PMN-PT (see Fig. 7d). However, for BFO grown on (111) PMN-30PT, the surface roughness was notably larger, over 30nm (see Fig. 7f). This resulted in the quality of the films to be not as good for (111) BFO, as for the other two orientations, at least as characterized by XRD.

• **<u>E-field controlled strain transition of BFO in BFO/PMN-PT heterostructures.</u>**

The crystal structure was then determined to be rhombohedral. Electric (E) fields were applied along the out-of-plane (OP) and in-plane (IP) directions, as shown in Figs. 10a and b. The maximum E applied was ±10kV/cm. The orientation and thickness of the thin films determined the IP strain of the BFO layer was modulated by E along both OP and IP directions. We found that the lattice parameters of BFO could be tuned by about 0.4% under E-field applied on PMN-PT. Butterfly-like strain vs E-field curves were observed in the BFO layer, transferred from the substrate, as shown in Figs. 10c and 10d. These results suggest the possibility to modulate the strain states of BFO along both OP and IP directions. One can thus expect the manipulation of the cycloidal-antiferromagnetic phase transition of BFO, as the strain state changes when crossing the magnetic phase boundaries.

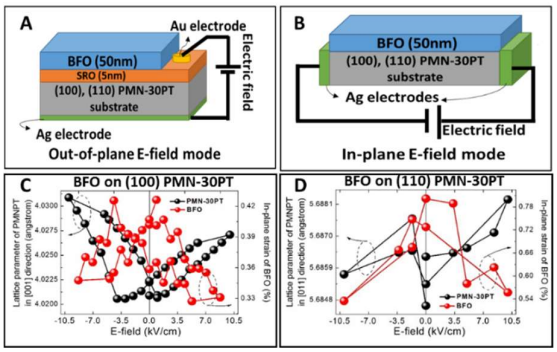

Figure 10. Schematic of BFO/PMN-30PT heterostructures in (a) OOP mode, and (b) IP mode. Butterfly-like strain vs E-field curves of BFO/PMN-30PT heterostructures, (c) (100) orientation, and (d) (110) orientation.

In addition, reciprocal space mapping (RSM) measurements revealed that applied electric fields (E) resulted in a change of the magnetic domain distribution in the BFO layer. These results clearly demonstrate important induced structural changes with application of E to the substrate. The structure of the PMN-PT substrate was found to be monoclinic A, as identified by fingerprint splitting patterns in the (011) mesh scans. Under application of 3kV/cm, changes in mesh scans were observed. Along the OP direction, as shown in Figs. 11b and 11d, shifts in the peak contours were found for both the substrate and BFO layer. Along the IP direction (see Figs. 11a and 11c), much more pronounced changes in the peak contours were found, demonstrating a switching of the domain structures in both substrate and BFO layer. In addition, in Figs 11e-g, atomic force (AFM), piezoelectric force (PFM), and magnetic force (MFM) microscopy images directly revealed switch of ferroelectric and magnetic domains in the BFO layer under a tip bias.

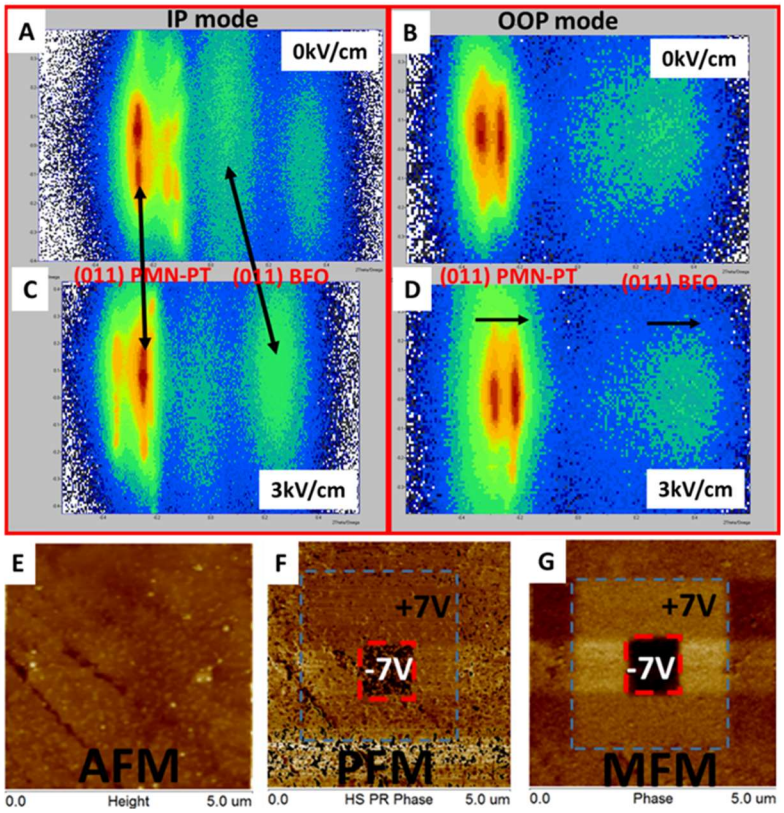

Figure 11. (011) RSM images of BFO/ PMNPT hetero-structures in (a) (c) IP mode, and (b) (d) OOP mode. (a) (b) at 0kV/cm E-field, (c) (d) at +3kV/cm E-field. (e) AFM height image, (f) PFM phase image, and (g) MFM phase image. The blue and red boxes point out the region poled by ±7kV/cm tip bias.

- **<u>E-controlled antiferromagnetic state changes in BFO/PMN-30PT</u>**

After optimizing the deposition conditions, 200-nm-thick BFO thin films were deposited on (001)-oriented PMN-30PT single crystal substrates (dimensions: 10cm×10cm) by pulsed laser deposition (PLD). Here, two different heterostructures were deposited and studied, labeled as Sample #1 and Sample #2. The film quality was checked by atomic force microscopy (AFM), x-ray diffraction (XRD), and P-E measurements.

An out-of-plane (OP) electric field E was *in-situ* applied across the PMN-PT substrates during XRD measurements. Figures 12a and 12c show 2theta scan patterns, from which the lattice parameters and strain were calculated according to Bragg's Law. As shown in Figure 12b and 12d, butterfly-like hysteresis loops demonstrate that the in plane (IP) strain of the BFO film was as a function of E applied along the OP. The data evidence that E applied on the PMN-PT substrate can reversibly tune the strain state of BFO, via elastic coupling at the interface. Differences in the data between Figs. 12b and 12d indicate that this tunability is notably dependent on the quality of the PMN-PT crystal substrates. The data indicate the possibility that the antiferromagnetic state of the BFO can also be modified by the external E.

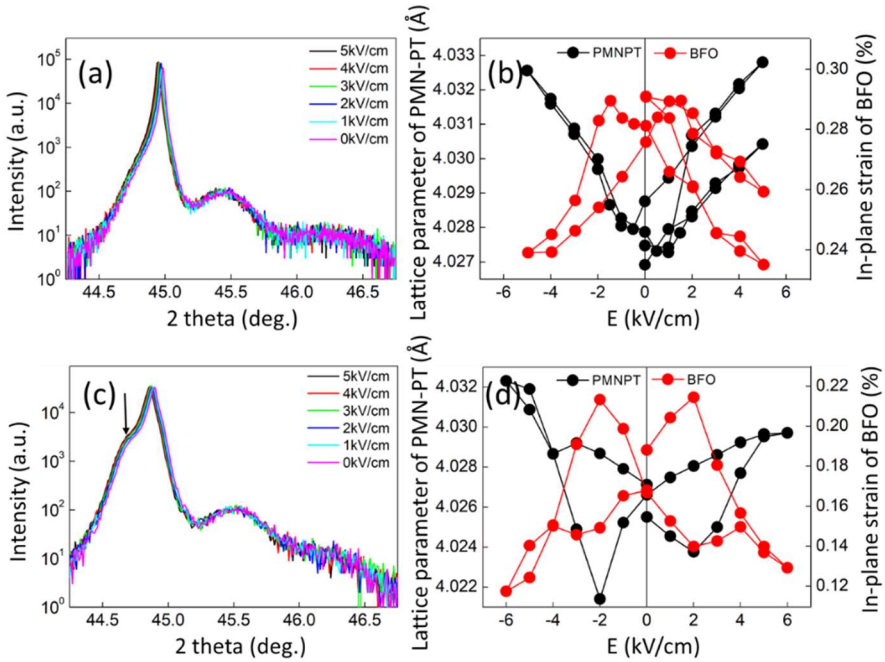

Figure 12. (a) (c) XRD 2theta scans patterns of (a) Sample #1, and (c) Sample #2. The calculated lattice parameter of PMN-PT and IP strain of BFO were plotted as a function as E in (b) and (d), respectively.

To study the antiferromagnetic (AFM) spin state of BFO and how it was altered by an applied E, neutron diffraction tests of Sample #1 were taken on the HB-1A line at Oak Ridge National Lab (ORNL) with the help of Dr. Wei Tian. Figure 13 shows mesh scans taken around the (0.5 0.5 0.5) reflection of BFO. These data indicate changes in the AFM state with increasing E from 0 kV/cm (Fig. 13a) to +4 kV/cm (Fig. 13b). A single peak representing a homogenious G-type AFM state was found for E=0kV/cm, which split into a doubled peak along the [1-10] direction under E=4 kV/cm. This splitting indicates an induced spin cycloid propagation along the [1-10].

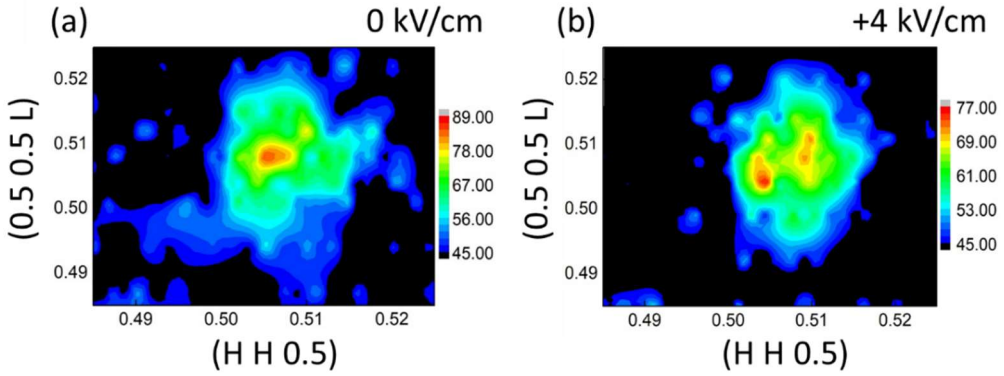

Figure 13. Neutron diffraction mesh scans of the Sample #1 around the (0.5 0.5 0.5) reflection. (a) at 0 kV/cm, (b) at +4 kV/cm. Measured by HB1-A at ORNL.

Figure 14a shows the mesh scans after E was removed, and then subsequently reapplied and increased again to E=9 kV/cm (Fig. 3b). Note that a change in collimation from 20'-20' to 40'-40' resulted in increased intensity in Figure 13 relative to Figure 12. When E was removed, the spin state partially reverted back to the G-type antiferromagnetic state, as the split peaks trended to merge together. The lack of a full recovery is probably due to the hysteretic nature of the induced stain of the piezoelectric PMN-30PT substrate, which did not completely return to its original state. Finally, when E>9 kV/cm, the peak split along the [11-2] direction, indicating an induced spin cycloid propagation along a different direction.

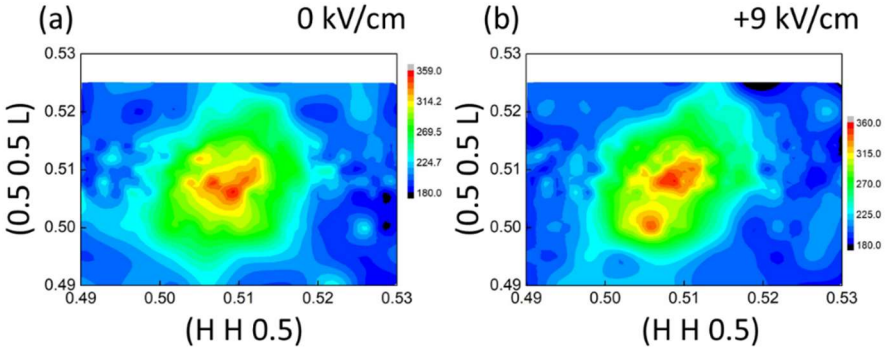

Figure 14. Neutron diffraction mesh scans of the Sample #1 around the (0.5 0.5 0.5) reflection. (a) at 0 kV/cm, (b) at +9 kV/cm. Measured by HB1-A at ORNL.

To confirm such an E-controlled AFM state change inside of the BFO layer, similar neutron diffraction mesh scans of Sample #2 were taken at the National Institute of Standard Technology (NIST) using BT-4 with the help of Dr. Alexander Grutter. As shown in Figure 15, peak splitting was not observed for Sample #2. Instead, the peak gradually shifted with increasing E, due to lattice changes of BFO elastically transferred from those induced by E applied to the PMN-PT substrate. Considering the butterfly-like curves in Figure 12 are different between Sample #1 and Sample #2, the neutron mesh scans indicate that changes in the AFM spin state may be notably dependent on the PMN-PT substrates quality. However, the possibility cannot be ruled out that the splitting in Sample #2 was too small to be detect by BT-4 at NIST. From the comparisons of the line scans in Figure 16 taken under 0kV/cm and 8kV/cm, one can clearly see that peak broadening occurs with increasing E.

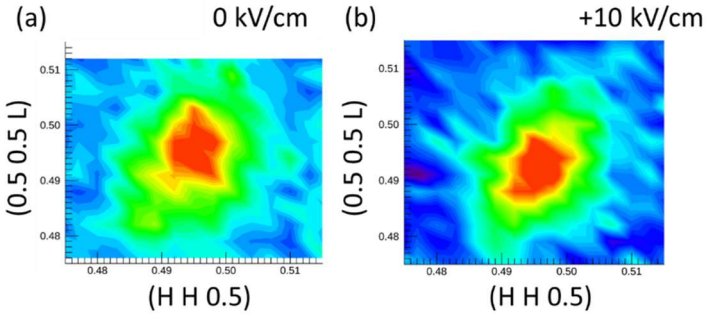

Figure 15. Neutron diffraction mesh scans of the Sample #2 around the (0.5 0.5 0.5) reflection. (a) at 0 kV/cm, (b) at +10 kV/cm. Measured by BT-4 at NIST.

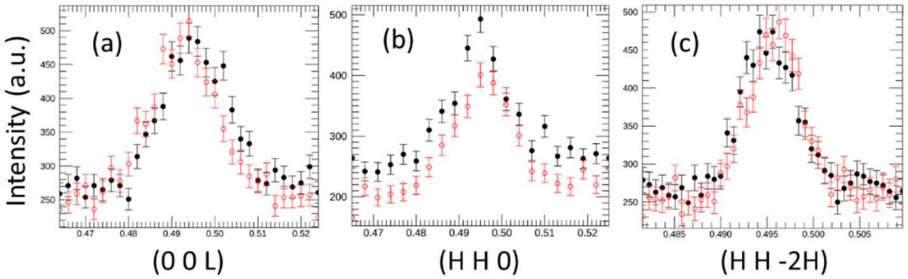

Figure 16. Neutron diffraction line scans of the Sample #2 sample around the (0.5 0.5 0.5) reflection. Black and red signs represent the data at 0 kV/cm and +10 kV/cm , respectively. (a) along the (0 0 L) zone, (b) along the (H H 0) zone, and (c) along the (H H -2H) zone. Measured by BT-4 at NIST.

4.4 **Nanocomposites of tetragonal phase CFO and BFO. (Viehland)**

Tetragonal phase CFO: CFO/BFO integrated nanocomposites were grown on $LaAlO_3$ substrates. It has previously been reported that the BFO phase in this case has a tetragonal structure. We obtained cross-sectional TEM images of our samples. As shown in Figures 17a-c, a platform-like self-assembled topography was found, which resulted from a discontinuity in the CFO phase distribution. We then performed selected area electron diffraction (SAED) studies which demonstrated that the structure of CFO was also tetragonal, when deposited on the T-phase BFO grown on $LaAlO_3$. To our knowledge, this is the first report of a T-phase CFO. This could have important ramifications to reducing the magnetic losses in ferrite thin layer magnetoelectrics.

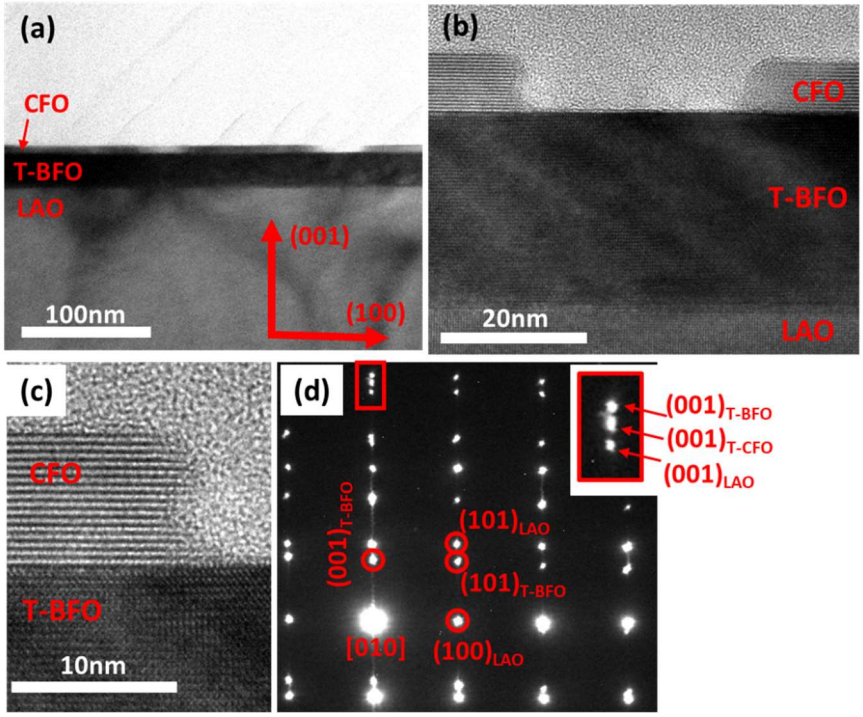

Figure 17. The cross-sectional TEM images of CFO(7nm)/T-phase BFO nanocomposite under different scales. The crystal orientation is shown in (a). (d) SAED patterns of (b). The zone axis is along [010] direction. The inset in (d) is the zoom-in image showing a triplet split along (001) orientation.

Changes in magnetic anisotropy of CFO/BFO on annealing: the effect of annealing on CFO/BFO heterostructure topography, crystal structure, and magnetic properties is summarized in Figure 18. The smooth as-grown sample surface (roughness of >1nm) developed into a specific self-assembled topography with increasing anneal time. This was accompanied by the strain relaxation in the x-ray diffraction patterns. Interestingly, the magnetic anisotropy was changed in the opposite way. This can be explained by a combination of shape, strain, and exchange coupling effects. Similar analysis was applied to the thickness effect in Figure 19. Such thermal tunability of the magnetic anisotropy of CFO/BFO heterostructures has previously not been reported, and offers an important way by which to control the magnetic and magnetoelectric properties and their dependence on orientation.

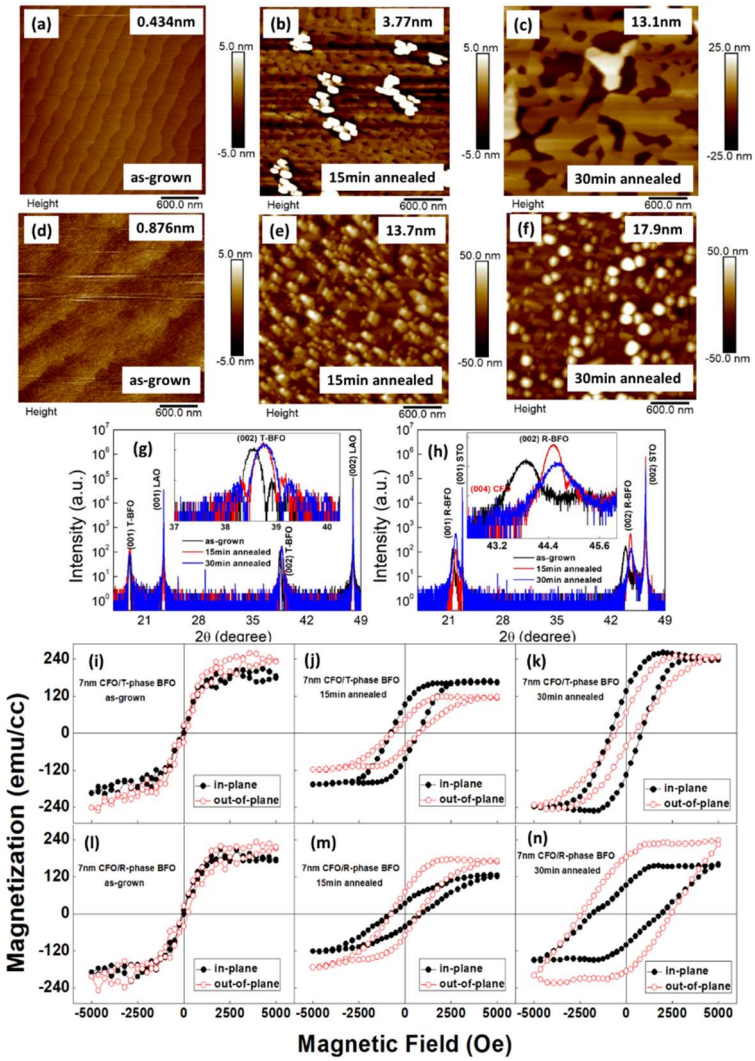

Figure 18. (a)-(f) AFM height images of (a)-(c) CFO(7nm)/BFO(28nm)/(001)LAO, and (d)–(f) CFO(7nm)/BFO(28nm)/(001)STO. The surface roughness is listed as insets. (g) (h) XRD patterns of (g) CFO(7nm)/BFO(28nm)/(001)LAO, and (h) CFO(7nm)/BFO(28nm)/(001)STO after different anneal processes. (i)-(n) Magnetic hysteresis loops of (i)-(k) CFO(7nm)/BFO(28nm)/(001)LAO, and (l)–(n) CFO(7nm)/BFO(28nm)/(001)STO. (a) (d) (i) (l) the as-grown samples, (b) (e) (j) (m) 15min annealed samples, and (c) (f) (k) (n) 30min annealed samples.

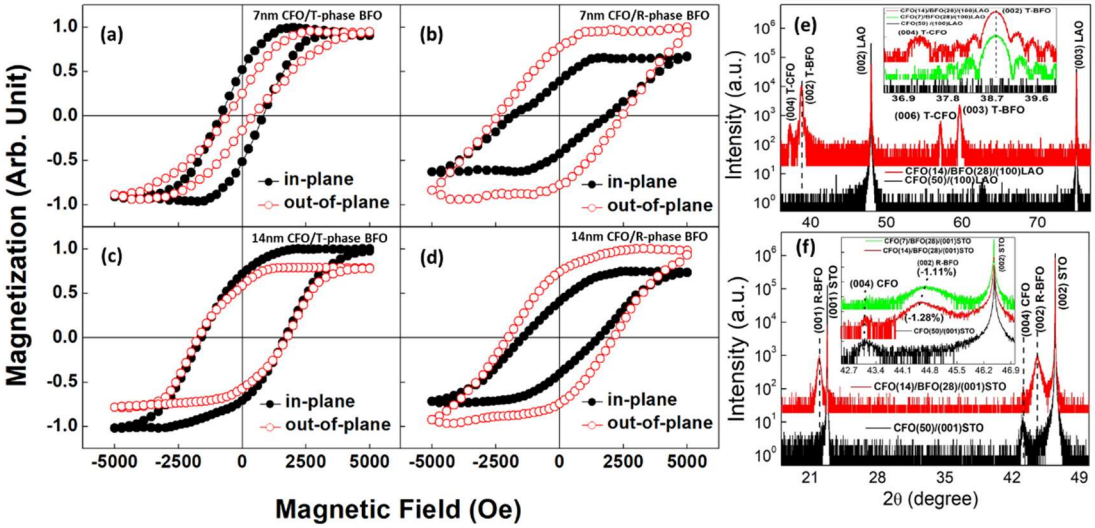

Figure 19. (a)–(d) Magnetic hysteresis loops of (a) (c) CFO/T-phase BFO on (001) LAO substrate, and (b) (d) CFO/R-phase BFO on (001) STO substrate. The thickness of CFO was 7nm in (a) (b), and 14nm in (c) (d). (e) (f) XRD patterns of (e) CFO/T-phase BFO nanocomposites, and (f) CFO/R-phase BFO nanocomposites. The insets in (e) (f) show the strain changes in CFO and BFO caused by a thickness factor.

Next, tetragonal structured BFO (T-phase BFO) and $CoFe_2O_4$ (CFO), CFO/T-phase BFO, nanocomposites were deposited on top of (001) $LaAlO_3$ (LAO) substrates. For comparisons, a control group CFO/R-phase BFO was deposited on (001) $SrTiO_3$ (STO). Although the CFO and BFO layers were deposited separately, after annealing at 725°C for 30min, the CFO top layer developed a self-assembled platform-like morphology with BFO on LAO (Fig. 20b). This phase distribution was different from the nanopillar CFO/R-phase BFO one previously reported on STO (Fig.20a). The AFM profile images of the CFO/T-phase showed that the platforms consisted of several different stage heights that were quite uniform with a roughness of <1nm. This will favor their integration with other functional thin films.

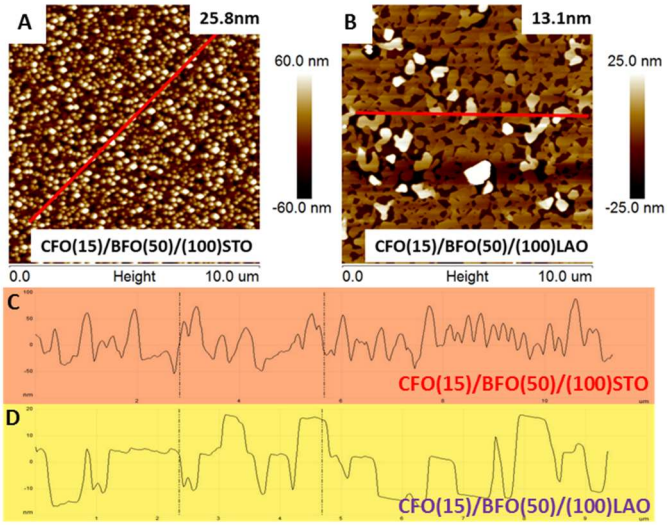

Figure 20. AFM height images of (a) CFO/R-phase BFO on STO, and (b) CFO/T-phase BFO on LAO. (c) and (d) are the profile images along the red lines in (a) and (b), respectively.

Magnetic force microscopy (MFM) images revealed that each CFO/T-phase platform contained multiple magnetic domains, whose distribution could be adjusted by applying a tip bias (see Figs. 21a and 21b). However, studies of the CFO/R-phase control group showed that each nanopillar remained as a single domain that barely changed under tip bias.

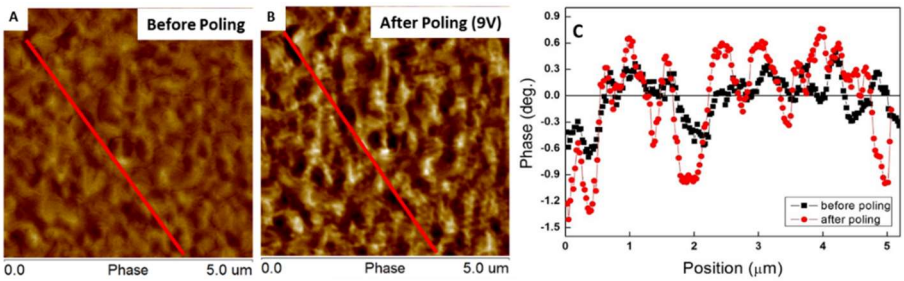

Figure 21. MFM phase images of CFO/T-phase platform structure. (a) Before and (b) after poled by a tip bias. (c) is the profile image along the red lines in (a) and (b).

5. A list of papers (already published, in press) in which DOE support is acknowledged.

Peer reviewed Journals: *(Provided by Priya)*

1) *Laser irradiation of Metal oxide Films and Nanostructures: Applications and Advances*, Haribabu Palneedi, Jung Hwan Park, Deepam Maurya, Mahesh Peddigari, Geon-Tae Hwang, Venkateswarlu Annapureddy, Jong-Woo Kim, Jong-Jin Choi, Byung-Dong Hahn, Shashank Priya, Keon Jae Lee, and Jungho Ryu. **Adv. Mater**. 30 (2018) 1705148
2) *Enhanced Self-Biased Magnetoelectric Coupling in Laser-Annealed Pb(Zr,Ti)O3 Thick Film Deposited on Ni Foil*, Haribabu Palneedi, Deepam Maurya, Liwei D. Geng, Hyun-Cheol Song , Geon-Tae Hwang, Mahesh Peddigari, Venkateswarlu Annapureddy, Kyung Song, Yoon Seok Oh, Su-Chul Yang, Yu U. Wang, Shashank Priya, and Jungho Ryu, **ACS Appl. Mater. Interfaces**, 2018, DOI: 10.1021/acsami.7b16706
3) *Surface Symmetry Effect on Self-Assembly of Three-Dimensional Single Crystal Piezoelectric Nanostructures,* Hyun-Cheol Song, Min-Gyu Kang, Deepam Maurya, Mohan Sanghadasa, Robert J. Bodnar, William T. Reynolds, Jr, and Shashank Priya, **Chem. Mater**., 30 (7), (2018), pp 2183–2187
4) *Magnetic Field Sensing by Exploiting Giant Nonstrain-Mediated Magnetodielectric Response in Epitaxial Composites,* Min Gyu Kang, Han Byul Kang, Michael Clavel, Deepam Maurya, Sreenivasulu Gollapudi, Mantu Hudait, Mohan Sanghadasa, and Shashank Priya*,* **Nano Lett**.*,* 2018*, DOI: 10.1021/acs.nanolett.7b05248,*
5) *High Power Magnetic Field Energy Harvesting Amplified Magneto-Mechanical Vibration,* Min Gyu Kang, Rammohan Sriramdas, Hyeon Lee, Jinsung Chun, Deepam Maurya, Geon Tae Hwang, Jungho Ryu, and Shashank Priya, **Advanced Energy Materials**, https://doi.org/10.1002/aenm.201703313 (In press, Feb. 2018)
6) *Soft mode phonon dynamics and phase transition in Aurivillius type structures,* Deepam Maurya, Ali Charkhesht, Sanjeev K. Nayak, Fu-Chang Sun, Deepu George, Abhijit Pramanick, Min-Gyu Kang, Hyun-Cheol Song, Marshall M. Alexander, Djamila Lou, Giti A. Khodaparast, S. Pamir Alpay, N. Q. Vinh, Shashank Priya, arXiv:1609.00859 [cond-mat.mtrl-sci] (Accepted for Publication in **Phys. Rev. B, 2017**).
7) *Unleashing the full potential of magnetoelectric coupling in film heterostructure*, H. Palneedi, D. Maurya, G.-Y. Kim, V. Annapureddy, M. S. Noh, C.-Y. Kang, J. -W. Kim, J.-J. Choi, S. -Y. Choi, S.-Y. Chung, S.-J. L. Kang, S. Priya, and J. Ryu, **Advanced Materials**, 2017, 29, 1605688.
8) *Compositionally Graded Multilayer Ceramic Capacitors,* Hyun-Cheol Song, Jie E. Zhou, Deepam Maurya, Yongke Yan, Yu U. Wang, and Shashank Priya*,* **Sci. Rep**.*, 7, (2017) 12353.*
9) *Wafer-Scale Single-Crystalline Ferroelectric Perovskite Nanorod Arrays,* Min Gyu Kang, Seul-Yi Lee, Deepam Maurya, Christopher Winkler, Hyun-Cheol Song, Robert B. Moore, Mohan Sanghadasa, and Shashank Priya*,* **Adv. Funct. Mater**.*, 27, (2017), 1701542.*
10) *Ultra-Low Resonant Piezoelectric MEMS Energy Harvester With High Power Density,* Hyun-Cheol Song, Prashant Kumar, Deepam Maurya, Min-Gyu Kang, William T. Reynolds, Dae-Yong Jeong, Chong-Yun Kang, Shashank Priya, **J. Microelectromech. Syst.,** 1057-7157, (2017), DOI: 10.1109/JMEMS.2017.2728821

11) *Enhanced piezoluminescence in non-stoichiometric ZnS:Cu microparticle based light emitting elastomers*, Jiayong Gan, Min Gyu Kang, Michael A. Meeker, Giti A. Khodaparast, Robert J. Bodnar, James E. Mahaney, Deepam Maurya, and Shashank Priya, **J. Mater. Chem. C**, 5, (2017) 5387-5394.
12) *Modulated Magneto-Thermal Response of $La_{0.85}Sr_{0.15}MnO_3$ and $(Ni_{0.6}Cu_{0.2}Zn_{0.2})Fe_2O_4$ Composites for Thermal Energy Harvesters,* Hyun-Cheol Song, Deepam Maurya, Jinsung Chun, Yuan Zhou, Myung-Eun Song, David Gray, Nana Kwame Yamoah, Dhananjay Kumar, Austin McDannald, Menka Jain, Shashank Priya*,* ***Energy Harvesting and System****, 2017, DOI: https://doi.org/10.1515/ehs-2016-0016.*
13) *Enhanced torsional actuation and stress coupling in Mn-modified $0.93(Na_{0.5}Bi_{0.5}TiO_3)$-$0.07BaTiO_3$ lead-free piezoceramic system*, Pelin Berik, Deepam Maurya, Prashant Kumar, Min Gyu Kang & Shashank Priya, **Science and Technology of Advanced Materials**, 2016, DOI: 10.1080/14686996.2016.1254569.
14) *Tailoring the Magnetoelectric Properties of $Pb(Zr,Ti)O_3$ Film Deposited on Amorphous Metglas Foil by Laser Annealing*, Haribabu Palneedi, Insung Choi, Gi-Yeop Kim, Venkateswarlu Annapureddy, Deepam Maurya, Shashank Priya, Jong-Woo Kim, Keon Jae Lee, Si-Young Choi, Sung-Yoon Chung, Suk-Joong L. Kang, and Jungho Ryu, **J. Am. Ceram. Soc**., 2016, 1–8, DOI: 10.1111/jace.14270.
15) *Giant Magnetoelectric Effect in PZT Thin Film Deposited on Nickel*, Reema Gupta, Monika Tomar, Vinay Gupta, Yuan Zhou, Anuj Chopra, Shashank Priya, A. S. Bhalla and R. Guo, **Energy Harvesting and Systems** 2016, 3(2), 181–188.
16) *Status and Perspectives of Multiferroic Magnetoelectric Composite Materials and Applications*, Haribabu Palneedi, Venkateswarlu Annapureddy, Shashank Priya, and Jungho Ryu, **Actuators**, 2016, 5(1), 9; doi:10.3390/act5010009.
17) *Self-Biased Magnetoelectric Composites: An Overview and Future Perspectives*, Yuan Zhou, Deepam Maurya, Yongke Yan, Gopalan Srinivasan, Eckhard Quandt, Shashank Priya, **Energy Harvesting and Systems**, 2015, 2329-8774, DOI: 10.1515/ehs-2015-0003.
18) *Enhanced off-resonance magnetoelectric response in laser annealed PZT thick film grown on magnetostrictive amorphous metal substrate*, Haribabu Palneedi, Deepam Maurya, Gi-Yeop Kim, Shashank Priya, Suk-Joong L. Kang, Kwang-Ho Kim, Si-Young Choi and Jungho Ryu, **Appl. Phys. Lett.** 2015, 107, 012904.
19) *Integration of lead-free ferroelectric thin films on HfO_2/Si (100) for high performance non-volatile memory applications*, S. Kundu, D. Maurya, D., M. Clavel, Y. Zhou, N. N. Halder, M. K. Hudait, P. Banerji, S. Priya, **Scientific Reports**, 2015, 5, 8494.
20) *Lead-free epitaxial ferroelectric material integration on semiconducting (100) Nb-doped $SrTiO_3$ for low-power non-volatile memory and efficient ultraviolet ray detection, S.* Kundu, M. Clavel, P. Biswas, B. Chen, H. -C. Song, P. Kumar, N. N. Halder, M. Hudait, P. Banerji, M. Sanghadasa, S. Priya, **Scientific Reports**, 2015, 5, 12415, DOi: 10.1038/srep12415.
21) *Integration of $SrTiO_3$ on Crystallographically Oriented Epitaxial Germanium for Low-power Device Applications*, M. K. Hudait, M. Clavel, Y. Zhu, P. Goley, S. Kundu, D. Maurya, and S. Priya, **ACS Appl. Mater. Interfaces**, 2015, 7 (9), pp 5471–5479.
22) *Cofired magnetoelectric transformer,*Yuan Zhou, Yongke Yan, and Shashank Priya, **Applied Physics Letters**, 104, 232906 (2014).
23) *Tensile-Strained Nanoscale Ge/In0.16Ga0.84As Heterostructure for Tunnel Field-Effect Transistor*, Yan Zhu, Deepam Maurya, Shashank Priya, and Mantu K. Hudait. **ACS Appl. Mater. Interfaces**, 6, 4947–4953 (2014).

Peer reviewed Journals: *(Provided by Viehland)*

Primary support

1. M. Gao, X. Tang, C.M. Leung, J.F. Li, and D. Viehland, "Phase transition and energy storage behavior of antiferroelectric PLZT thin films epitaxially deposited on SRO buffered STO single

crystal substrates", Journal of the American Ceramic Society, Volume: 102, Issue: 9, Pages: 5180-5191 (Sept. 2019).
[Work was part of Min Gao's PhD thesis. It was primarily his work and he was supported by this DOE grant. Xiao Tang gave supplementary support in some TEM measurements, and he was supported by AFOSR].

2. M. Gao, X. Tang, S. Dai, J.F. Li, and D. Viehland, "Depth dependent ferroelectric to incommensurate/commensurate antiferroelectric phase transition in epitaxial lanthanum modified lead zirconate titanate thin films", Applied Physics Letters, Vol: 115, Issue: 7, Article Number: 072901 (August 2019).
[Work was part of Min Gao's PhD thesis. It was primarily his work and he was supported by this DOE grant. Xiao Tang gave supplementary support in some TEM measurements, and he was supported by AFOSR].
3. M. Gao, R. Viswan, X. Tang, C. Leung, J.F. Li, and D. Viehland, "Magnetoelectricity of CoFe2O4 and tetragonal phase BiFeO3 nanocomposites prepared by pulsed laser deposition", SCIENTIFIC REPORTS Volume: 8, Article Number: 323, DOI: 10.1038/s41598-017-18788-8, Published:JAN 10 2018.
[Work was part of Min Gao's PhD thesis. It was primarily his work and he was supported by this DOE grant. Xiao Tang gave supplementary support in some TEM measurements, and he was supported by AFOSR].
4. M. Gao, R. Viswan, X. Tang, C. Leung, J.F. Li, and D. Viehland, "E-field controlled phase transformation in bismuth ferrite thin films, and effect of laser energy density", APPLIED PHYSICS LETTERS **Volume:** 111, **Issue:** 15, **Article Number:** 152905, **DOI:** 10.1063/1.4997017 (Oct. 2017).
[Work was part of Min Gao's PhD thesis. It was primarily his work and he was supported by this DOE grant. Xiao Tang gave supplementary support in some TEM measurements, and he was supported by AFOSR].
5. Z. Wang, Y. Wang, H. Luo, J.F. Li, and D. Viehland, "Crafting the strain state in epitaxial thin films: A case study of CoFe2O4 films on Pb(Mg,Nb)O-3-PbTiO3", PHYSICAL REVIEW B, Volume: 90, Issue: 13, Article Number: 134103, DOI: 10.1103/PhysRevB.90.134103 (2014).
6. M. Gao, X. Tang, W. Tian, et al. Strain-mediated electric field manipulation of the antiferromagnetic state in BiFeO3/Pb(Mg1/3Nb2/3)O3-PbTiO3 heterostructures. (in submission process).

Partial support (Review Paper).

7. D. Viehland and E.K.H. Salje, "Domain boundary-dominated systems: adaptive structures and functional twin boundaries", ADVANCES IN PHYSICS, Volume: 63, Issue: 4, Pages: 267-326, DOI: 10.1080/00018732.2014. 974304 (2014).
[This was a review paper of the authors work over many years, part of work was supported by this DOE grant].

Book Chapters:

1) *Applications of Multiferroic Magnetoelectric Composites* in Multiferroic Materials: Properties, Techniques, and Applications (Edited by Junling Wang), Yuan Zhou, Jong-Woo Kim, Shuxiang Dong, Shashank Priya, Junling Wang, and Jungho Ryu, Taylor & Francis Group, Ch. 8, pages 215-254, 2016, DOI: 10.1201/9781315372532-9.
2) *Recent advances in piezoelectric and magnetostrictive materials and phenomena* in Composite Magnetoelectrics: Materials, Structures, and Applications (Editor: G Srinivasan, S Priya, N Sun), Shashank Priya, Su Chul Yang, Deepam Maurya, Yongke Yan, Woodhead publishing, Ch. 6, page 103-153, 2015.

6. A list of people working on the project -graduate students, postdocs, visitors, technicians, etc. Indicate for each whether receiving full or partial support. In case of partial support indicate percentage of support.

With Priya
Deepam Maurya
Min Gyu Kang
Ram Mohan Sriramdas

With Viehland
Min Gao

8. An update list of other support (current and pending, federal and non-federal.) For each, indicate the overlap, if any, and/or distinctiveness with the DOE-supported project. This could be brief -one or two sentences.

<u>Current and Pending (S. Priya)</u>

Current and Pending Support

(See PAPPG Section II.C.2.h for guidance on information to include on this form.)

The following information should be provided for each investigator and other senior personnel. Failure to provide this information may delay consideration of this proposal.

Investigator: Shashank Priya

Other agencies (including NSF) to which this proposal has been/will be submitted.

Support: ☒ Current ☐ Pending ☐ Submission Planned in Near Future ☐ *Transfer of Support
Project/Proposal Title: Nano Engineered Thermoelectric Systems (NETS) for Lightweight Portable Primary/Secondary Power Sources
Source of Support: DARPA
Total Award Amount: $ 548,750 Total Award Period Covered: 12/18/17 - 12/10/19
Location of Project: The Pennsylvania State University
Person-Months Per Year Committed to the Project. Cal:0.48 Acad: 0.00 Sumr: 0.00

Support: ☒ Current ☐ Pending ☐ Submission Planned in Near Future ☐ *Transfer of Support
Project/Proposal Title: Tunable Energy Efficient Electronics (TE3)
Source of Support: DARPA
Total Award Amount: $ 3,998,874 Total Award Period Covered: 09/01/15 - 12/31/19
Location of Project: Virginia Tech
Person-Months Per Year Committed to the Project. Cal:0.00 Acad: 0.45 Sumr: 0.90

Support: ☒ Current ☐ Pending ☐ Submission Planned in Near Future ☐ *Transfer of Support
Project/Proposal Title: PFI: AIR-TT: Textured Piezoelectric Ceramics
Source of Support: National Science Foundation
Total Award Amount: $ 199,999 Total Award Period Covered: 01/02/18 - 12/31/19
Location of Project: The Pennsylvania State University
Person-Months Per Year Committed to the Project. Cal:0.48 Acad: 0.00 Sumr: 0.00

Support: ☒ Current ☐ Pending ☐ Submission Planned in Near Future ☐ *Transfer of Support
Project/Proposal Title: SBIR - High ZT Module Development and Optimized Thermal Interfaces
Source of Support: SA Photonics
Total Award Amount: $ 390,000 Total Award Period Covered: 06/01/16 - 01/10/20
Location of Project: Virginia Tech
Person-Months Per Year Committed to the Project. Cal:0.39 Acad: 0.00 Sumr: 0.00

Support: ☒ Current ☐ Pending ☐ Submission Planned in Near Future ☐ *Transfer of Support
Project/Proposal Title: Mesoscale Design of Magnetoelectric Heterostructures and Nanocomposites
Source of Support: DOE
Total Award Amount: $ 520,610 Total Award Period Covered: 08/01/15 - 12/31/19
Location of Project: Virginia Tech
Person-Months Per Year Committed to the Project. Cal:0.00 Acad: 0.18 Summ: 0.15

*If this project has previously been funded by another agency, please list and furnish information for immediately preceding funding period.

Page G-1 USE ADDITIONAL SHEETS AS NECESSARY

Current and Pending Support

(See PAPPG Section II.C.2.h for guidance on information to include on this form.)

The following information should be provided for each investigator and other senior personnel. Failure to provide this information may delay consideration of this proposal.

Investigator: Shashank Priya

Other agencies (including NSF) to which this proposal has been/will be submitted.

Support: ☒ Current ☐ Pending ☐ Submission Planned in Near Future ☐ *Transfer of Support
Project/Proposal Title: Phase 2 IUCRC Virginia Tech: Center for Energy Harvesting Materials and Systems (CEHMS)

Source of Support: National Science Foundation
Total Award Amount: $ 320,000 Total Award Period Covered: 08/01/17 - 07/31/22
Location of Project: Virginia Tech
Person-Months Per Year Committed to the Project. Cal:0.01 Acad: 0.00 Sumr: 0.00

Support: ☒ Current ☐ Pending ☐ Submission Planned in Near Future ☐ *Transfer of Support
Project/Proposal Title: MRI Consortium: Development of Instrumentation for the PICO-500 Bubble Chamber

Source of Support: NSF
Total Award Amount: $ 109,862 Total Award Period Covered: 09/15/18 - 08/31/21
Location of Project: The Pennsylvania State University
Person-Months Per Year Committed to the Project. Cal:0.32 Acad: 0.00 Sumr: 0.00

Support: ☒ Current ☐ Pending ☐ Submission Planned in Near Future ☐ *Transfer of Support
Project/Proposal Title: IRES Track III: Penn State - American Ceramics Society - University of Kiel (PACK) International Research Experience Fellowship

Source of Support: National Science Foundation
Total Award Amount: $ 500,000 Total Award Period Covered: 09/01/18 - 08/31/21
Location of Project: The Pennsylvania State University
Person-Months Per Year Committed to the Project. Cal:0.33 Acad: 0.00 Sumr: 0.00

Support: ☒ Current ☐ Pending ☐ Submission Planned in Near Future ☐ *Transfer of Support
Project/Proposal Title: NRI: INT: COLLAB: Rumen Understanding through Millipede-Engineered Navigation and Sensing (RUMENS)

Source of Support: United States Department of Agriculture
Total Award Amount: $ 500,000 Total Award Period Covered: 03/01/19 - 02/28/23
Location of Project: The Pennsylvania State University
Person-Months Per Year Committed to the Project. Cal:0.38 Acad: 0.00 Sumr: 0.00

Support: ☒ Current ☐ Pending ☐ Submission Planned in Near Future ☐ *Transfer of Support
Project/Proposal Title: Biophysical investigations on additive manufactured nanoscale biosensors and biological materials

Source of Support: AFOSR
Total Award Amount: $ 750,000 Total Award Period Covered: 07/15/18 - 12/14/20
Location of Project: The Pennsylvania State University
Person-Months Per Year Committed to the Project. Cal:0.60 Acad: 0.00 Summ: 0.00

*If this project has previously been funded by another agency, please list and furnish information for immediately preceding funding period.

Page G-2 USE ADDITIONAL SHEETS AS NECESSARY

Current and Pending Support

(See PAPPG Section II.C.2.h for guidance on information to include on this form.)

The following information should be provided for each investigator and other senior personnel. Failure to provide this information may delay consideration of this proposal.

Investigator: Shashank Priya

Other agencies (including NSF) to which this proposal has been/will be submitted.

Support: ☒ Current ☐ Pending ☐ Submission Planned in Near Future ☐ *Transfer of Support
Project/Proposal Title: Low-Temperature Fabrication of Flexible, High Efficiency Perovskite Photovoltaic Modules for Energy Harvesting Applications
Source of Support: NanoSonic, Inc
Total Award Amount: $ 500,000 Total Award Period Covered: 09/25/18 - 09/25/20
Location of Project: The Pennsylvania State University
Person-Months Per Year Committed to the Project. Cal:0.36 Acad: 0.00 Sumr: 0.00

Support: ☒ Current ☐ Pending ☐ Submission Planned in Near Future ☐ *Transfer of Support
Project/Proposal Title: Tunable Textured Composites for Lightweight Power Systems
Source of Support: QorTek
Total Award Amount: $ 400,000 Total Award Period Covered: 11/19/18 - 09/18/20
Location of Project: The Pennsylvania State University
Person-Months Per Year Committed to the Project. Cal:0.37 Acad: 0.00 Sumr: 0.00

Support: ☒ Current ☐ Pending ☐ Submission Planned in Near Future ☐ *Transfer of Support
Project/Proposal Title: Planning Grant: Engineering Research Center for Wireless Power (WiPOWER) for a Cordless World
Source of Support: National Science Foundation
Total Award Amount: $ 100,000 Total Award Period Covered: 09/01/18 - 08/31/20
Location of Project: The Pennsylvania State University
Person-Months Per Year Committed to the Project. Cal:0.15 Acad: 0.00 Sumr: 0.00

Support: ☒ Current ☐ Pending ☐ Submission Planned in Near Future ☐ *Transfer of Support
Project/Proposal Title: Textured Piezoelectrics Tailored for High Power Acoustic Transduction
Source of Support: Defense Advanced Research Projects Agency
Total Award Amount: $ 627,170 Total Award Period Covered: 11/01/18 - 10/31/20
Location of Project: The Pennsylvania State University
Person-Months Per Year Committed to the Project. Cal:0.42 Acad: 0.00 Sumr: 0.00

Support: ☐ Current ☒ Pending ☐ Submission Planned in Near Future ☐ *Transfer of Support
Project/Proposal Title: Piezoluminescence: Controlled conversion of mechanical energy into light
Source of Support: Army Research Office
Total Award Amount: $ 353,130 Total Award Period Covered: 09/01/18 - 08/31/21
Location of Project: The Pennsylvania State University
Person-Months Per Year Committed to the Project. Cal:0.36 Acad: 0.00 Summ: 0.00

*If this project has previously been funded by another agency, please list and furnish information for immediately preceding funding period.

Page G-3 USE ADDITIONAL SHEETS AS NECESSARY

Current and Pending Support

(See PAPPG Section II.C.2.h for guidance on information to include on this form.)

The following information should be provided for each investigator and other senior personnel. Failure to provide this information may delay consideration of this proposal.

Investigator: Shashank Priya

Other agencies (including NSF) to which this proposal has been/will be submitted.

Support: ☐ Current ☒ Pending ☐ Submission Planned in Near Future ☐ *Transfer of Support
Project/Proposal Title: Laser and Photonic Sintering for Ultrafast Synthesis of Multifunctional Materials with Novel Microstructures

Source of Support: U.S. Department of the Navy
Total Award Amount: $ 198,300 Total Award Period Covered: 06/15/19 - 06/14/20
Location of Project: The Pennsylvania State University
Person-Months Per Year Committed to the Project. Cal:0.00 Acad: 0.00 Sumr: 0.00

Support: ☒ Current ☐ Pending ☐ Submission Planned in Near Future ☐ *Transfer of Support
Project/Proposal Title: On-Demand Adaptive Power for UAVs

Source of Support: U.S. Army Research, Development and Engineering Command
Total Award Amount: $ 1,000,000 Total Award Period Covered: 09/16/19 - 08/16/21
Location of Project: The Pennsylvania State University
Person-Months Per Year Committed to the Project. Cal:0.54 Acad: 0.00 Sumr: 0.00

Support: ☐ Current ☒ Pending ☐ Submission Planned in Near Future ☐ *Transfer of Support
Project/Proposal Title: Orthopedic Implant Prototype

Source of Support: RTI International
Total Award Amount: $ 50,000 Total Award Period Covered: 02/01/19 - 07/31/19
Location of Project: The Pennsylvania State University
Person-Months Per Year Committed to the Project. Cal:0.06 Acad: 0.00 Sumr: 0.00

Support: ☒ Current ☐ Pending ☐ Submission Planned in Near Future ☐ *Transfer of Support
Project/Proposal Title: CREST Center for Renewable Energy and Advanced Materials (CREAM)

Source of Support: Norfolk State University
Total Award Amount: $ 150,000 Total Award Period Covered: 07/15/18 - 06/30/21
Location of Project: The Pennsylvania State University
Person-Months Per Year Committed to the Project. Cal:0.24 Acad: 0.00 Sumr: 0.00

Support: ☒ Current ☐ Pending ☐ Submission Planned in Near Future ☐ *Transfer of Support
Project/Proposal Title: CREST Center for Renewable Energy and Advanced Materials (CREAM)

Source of Support: Norfolk State University
Total Award Amount: $ 150,000 Total Award Period Covered: 07/15/18 - 06/30/21
Location of Project: The Pennsylvania State University
Person-Months Per Year Committed to the Project. Cal:0.24 Acad: 0.00 Sumr: 0.00

Support: ☐ Current ☒ Pending ☐ Submission Planned in Near Future ☐ *Transfer of Support
Project/Proposal Title: High-efficiency Low-temperature gradient SMA heat engine

Source of Support: M-Mech Defense, Inc
Total Award Amount: $ 49,930 Total Award Period Covered: 03/25/19 - 01/24/20
Location of Project: The Pennsylvania State University
Person-Months Per Year Committed to the Project. Cal:0.06 Acad: 0.00 Summ: 0.00

*If this project has previously been funded by another agency, please list and furnish information for immediately preceding funding period.

 USE ADDITIONAL SHEETS AS NECESSARY

Current and Pending Support

(See PAPPG Section II.C.2.h for guidance on information to include on this form.)

The following information should be provided for each investigator and other senior personnel. Failure to provide this information may delay consideration of this proposal.

Investigator: Shashank Priya

Other agencies (including NSF) to which this proposal has been/will be submitted.

Support: ☒ Current ☐ Pending ☐ Submission Planned in Near Future ☐ *Transfer of Support
Project/Proposal Title: Shape Memory Alloy Heat Engine

Source of Support: NextGen Aeronautics, Inc
Total Award Amount: $ 45,000 Total Award Period Covered: 04/01/19 - 01/30/20
Location of Project: The Pennsylvania State University
Person-Months Per Year Committed to the Project. Cal:0.06 Acad: 0.00 Sumr: 0.00

Support: ☒ Current ☐ Pending ☐ Submission Planned in Near Future ☐ *Transfer of Support
Project/Proposal Title: Towards Internet of Implantable Things: A Micro-Scale Magnetoelectric Intra-Body Communication Platform

Source of Support: National Science Foundation
Total Award Amount: $ 428,540 Total Award Period Covered: 08/01/19 - 07/31/22
Location of Project: The Pennsylvania State University
Person-Months Per Year Committed to the Project. Cal:0.12 Acad: 0.00 Sumr: 0.00

Support: ☒ Current ☐ Pending ☐ Submission Planned in Near Future ☐ *Transfer of Support
Project/Proposal Title: CPS: Closed Loop Sustainable Preci

Source of Support: Virginia Polytechnic Institute and State University (USDA)
Total Award Amount: $ 179,139 Total Award Period Covered: 08/01/18 - 07/14/21
Location of Project: The Pennsylvania State University
Person-Months Per Year Committed to the Project. Cal:0.12 Acad: 0.00 Sumr: 0.00

Support: ☒ Current ☐ Pending ☐ Submission Planned in Near Future ☐ *Transfer of Support
Project/Proposal Title: Unmanned aerial system with infinite energy scavenging

Source of Support: NanoSonic, Inc
Total Award Amount: $ 42,000 Total Award Period Covered: 06/03/19 - 12/09/19
Location of Project: The Pennsylvania State University
Person-Months Per Year Committed to the Project. Cal:0.06 Acad: 0.00 Sumr: 0.00

Support: ☒ Current ☐ Pending ☐ Submission Planned in Near Future ☐ *Transfer of Support
Project/Proposal Title: Electrospray Deposition of Perovskite Solar Cells

Source of Support: NanoSonic, Inc
Total Award Amount: $ 75,000 Total Award Period Covered: 07/01/19 - 03/31/20
Location of Project: The Pennsylvania State University
Person-Months Per Year Committed to the Project. Cal:0.09 Acad: 0.00 Summ: 0.00

*If this project has previously been funded by another agency, please list and furnish information for immediately preceding funding period.

Page G-5 USE ADDITIONAL SHEETS AS NECESSARY

Current and Pending Support

(See PAPPG Section II.C.2.h for guidance on information to include on this form.)

The following information should be provided for each investigator and other senior personnel. Failure to provide this information may delay consideration of this proposal.

Investigator: Shashank Priya

Other agencies (including NSF) to which this proposal has been/will be submitted.

Support: ☒ Current ☐ Pending ☐ Submission Planned in Near Future ☐ *Transfer of Support
Project/Proposal Title: High-Power-Density High-Efficiency Carbon Nanotube Thermo-Acoustic (TA) Projectors

Source of Support: Office of Naval Research
Total Award Amount: $ 375,000 Total Award Period Covered: 06/15/19 - 06/14/22
Location of Project: The Pennsylvania State University
Person-Months Per Year Committed to the Project. Cal:0.12 Acad: 0.00 Sumr: 0.00

Support: ☐ Current ☒ Pending ☐ Submission Planned in Near Future ☐ *Transfer of Support
Project/Proposal Title: Energy Efficient Material Processing through Automated Process Monitoring and Controls

Source of Support: Virginia Tech (DOE)
Total Award Amount: $ 126,750 Total Award Period Covered: 01/01/19 - 09/30/20
Location of Project: The Pennsylvania State University
Person-Months Per Year Committed to the Project. Cal:0.48 Acad: 0.00 Sumr: 0.00

Support: ☐ Current ☒ Pending ☐ Submission Planned in Near Future ☐ *Transfer of Support
Project/Proposal Title: Synthetic Aperture by Direct Print-down of Micro-lens Arrays on CMOS Imagers

Source of Support: NanoSonic, Inc
Total Award Amount: $ 33,500 Total Award Period Covered: 01/01/20 - 10/31/20
Location of Project: The Pennsylvania State University
Person-Months Per Year Committed to the Project. Cal:0.03 Acad: 0.00 Sumr: 0.00

Support: ☐ Current ☒ Pending ☐ Submission Planned in Near Future ☐ *Transfer of Support
Project/Proposal Title: Power Generation for Individual Soldier

Source of Support: NanoSonic, Inc
Total Award Amount: $ 33,500 Total Award Period Covered: 01/01/20 - 10/31/20
Location of Project: The Pennsylvania State University
Person-Months Per Year Committed to the Project. Cal:0.03 Acad: 0.00 Sumr: 0.00

Support: ☐ Current ☒ Pending ☐ Submission Planned in Near Future ☐ *Transfer of Support
Project/Proposal Title: Additive Manufacturing of Inorganic Transparent Materials for Advanced Optics

Source of Support: NanoSonic, Inc
Total Award Amount: $ 68,000 Total Award Period Covered: 01/01/20 - 12/31/20
Location of Project: The Pennsylvania State University
Person-Months Per Year Committed to the Project. Cal:0.12 Acad: 0.00 Summ: 0.00

*If this project has previously been funded by another agency, please list and furnish information for immediately preceding funding period.

Page G-6 USE ADDITIONAL SHEETS AS NECESSARY

Current and Pending Support

(See PAPPG Section II.C.2.h for guidance on information to include on this form.)

The following information should be provided for each investigator and other senior personnel. Failure to provide this information may delay consideration of this proposal.

Investigator: Shashank Priya

Other agencies (including NSF) to which this proposal has been/will be submitted.

Support: ☒ Current ☐ Pending ☐ Submission Planned in Near Future ☐ *Transfer of Support
Project/Proposal Title: Lead-free Radio-pure Textured Piezoelectric Ceramics for Acoustic Sensors in Dark Matter Search

Source of Support: National Science Foundation
Total Award Amount: $ 480,000 Total Award Period Covered: 01/01/20 - 12/31/22
Location of Project: The Pennsylvania State University
Person-Months Per Year Committed to the Project. Cal:0.12 Acad: 0.00 Sumr: 0.00

Support: ☒ Current ☐ Pending ☐ Submission Planned in Near Future ☐ *Transfer of Support
Project/Proposal Title: Planning Grant: Engineering Research Center for Thermal Energy Recovery, Refrigeration and Management (TERRM)

Source of Support: National Science Foundation
Total Award Amount: $ 100,000 Total Award Period Covered: 09/01/19 - 08/31/20
Location of Project: The Pennsylvania State University
Person-Months Per Year Committed to the Project. Cal:0.12 Acad: 0.00 Sumr: 0.00

Support: ☐ Current ☒ Pending ☐ Submission Planned in Near Future ☐ *Transfer of Support
Project/Proposal Title: Planning Grant: Engineering Research Center for Ubiquitous Wireless Power for a Healthy World

Source of Support: National Science Foundation
Total Award Amount: $ 100,000 Total Award Period Covered: 08/01/19 - 07/31/20
Location of Project: The Pennsylvania State University
Person-Months Per Year Committed to the Project. Cal:0.00 Acad: 0.00 Sumr: 0.00

Support: ☐ Current ☒ Pending ☐ Submission Planned in Near Future ☐ *Transfer of Support
Project/Proposal Title: Multi-functional Energy Harvester for Unmanned Aerial Vehicles

Source of Support: M-Mech Defense, Inc
Total Award Amount: $ 490,000 Total Award Period Covered: 01/01/20 - 12/31/21
Location of Project: The Pennsylvania State University
Person-Months Per Year Committed to the Project. Cal:0.36 Acad: 0.00 Sumr: 0.00

Support: ☒ Current ☐ Pending ☐ Submission Planned in Near Future ☐ *Transfer of Support
Project/Proposal Title: Nonlinear and Terahertz Studies of Electro-Optic and Magneto-Electric Materials

Source of Support: Virginia Polytechnic Institute and State University (USDA)
Total Award Amount: $ 93,335 Total Award Period Covered: 04/01/09 - 09/14/20
Location of Project: The Pennsylvania State University
Person-Months Per Year Committed to the Project. Cal:0.12 Acad: 0.00 Summ: 0.00

*If this project has previously been funded by another agency, please list and furnish information for immediately preceding funding period.

 USE ADDITIONAL SHEETS AS NECESSARY

Current and Pending Support

(See PAPPG Section II.C.2.h for guidance on information to include on this form.)

The following information should be provided for each investigator and other senior personnel. Failure to provide this information may delay consideration of this proposal.

Investigator: Shashank Priya

Other agencies (including NSF) to which this proposal has been/will be submitted.

Support: ☐ Current ☒ Pending ☐ Submission Planned in Near Future ☐ *Transfer of Support
Project/Proposal Title: High-throughput Machine-learning-based Design and Manufacturing of Cost-effective Thermoelectric Materials and Modules with 15% Efficiency
Source of Support: U.S Department of Energy
Total Award Amount: $ 3,999,203 Total Award Period Covered: 03/01/20 - 02/28/23
Location of Project: The Pennsylvania State University
Person-Months Per Year Committed to the Project. Cal:0.60 Acad: 0.00 Sumr: 0.00

Support: ☐ Current ☒ Pending ☐ Submission Planned in Near Future ☐ *Transfer of Support
Project/Proposal Title: Catalyzing Sustainable Precision Animal Agriculture
Source of Support: USDA National Institute of Food and Agriculture
Total Award Amount: $ 3,200,449 Total Award Period Covered: 06/01/20 - 05/31/25
Location of Project: The Pennsylvania State University
Person-Months Per Year Committed to the Project. Cal:0.60 Acad: 0.00 Sumr: 0.00

Support: ☐ Current ☒ Pending ☐ Submission Planned in Near Future ☐ *Transfer of Support
Project/Proposal Title: GLIde-Matched Electrocaloric Refrigeration (GLIMER)
Source of Support: U.S Department of Energy
Total Award Amount: $ 2,499,808 Total Award Period Covered: 04/01/20 - 03/31/23
Location of Project: The Pennsylvania State University
Person-Months Per Year Committed to the Project. Cal:0.12 Acad: 0.00 Sumr: 0.00

Support: ☒ Current ☐ Pending ☐ Submission Planned in Near Future ☐ *Transfer of Support
Project/Proposal Title: IUCRC Phase II IUCRC Renewal Center for Energy Harvesting Materials and Systems (CEHMS) Virginia Tech
Source of Support: Virginia Tech (NSF)
Total Award Amount: $ 40,000 Total Award Period Covered: 08/01/19 - 07/31/20
Location of Project: The Pennsylvania State University
Person-Months Per Year Committed to the Project. Cal:0.12 Acad: 0.00 Sumr: 0.00

Support: ☐ Current ☒ Pending ☐ Submission Planned in Near Future ☐ *Transfer of Support
Project/Proposal Title: Quantum Spectrally-Enhanced Self-Powered Artificial Retina
Source of Support: AFOSR
Total Award Amount: $ 687,423 Total Award Period Covered: 01/01/20 - 12/31/22
Location of Project: The Pennsylvania State University
Person-Months Per Year Committed to the Project. Cal:0.12 Acad: 0.00 Summ: 0.00

*If this project has previously been funded by another agency, please list and furnish information for immediately preceding funding period.

Page G-8 USE ADDITIONAL SHEETS AS NECESSARY

Current and Pending Support

(See PAPPG Section II.C.2.h for guidance on information to include on this form.)

The following information should be provided for each investigator and other senior personnel. Failure to provide this information may delay consideration of this proposal.

Investigator: Shashank Priya

Other agencies (including NSF) to which this proposal has been/will be submitted.

Support: ☐ Current ☒ Pending ☐ Submission Planned in Near Future ☐ *Transfer of Support

Project/Proposal Title: EFRI DCheM Preliminary Proposal: Distributed Ammonia Synthesis with Hierarchical Energy Devices (DASHED)

Source of Support: Virginia Tech (NSF)

Total Award Amount: $ 392,000 Total Award Period Covered: 07/01/20 - 06/30/24

Location of Project: The Pennsylvania State University

Person-Months Per Year Committed to the Project. Cal: 1.00 Acad: 0.00 Sumr: 0.00

Support: ☐ Current ☐ Pending ☐ Submission Planned in Near Future ☐ *Transfer of Support

Project/Proposal Title:

Source of Support:

Total Award Amount: $ Total Award Period Covered:

Location of Project:

Person-Months Per Year Committed to the Project. Cal: Acad: Sumr:

Current and Pending (D. Viehland, as of June 2019)

Investigator: Dwight Viehland	Other Agencies to which this proposal has been/will be submitted:
Support (Current, Pending, Submission Planned in Future or Transfer of Support): Current	
Project/Proposal Title and grant number, if appropriate: Magnetic Sensors for Detection Award number: N00014-15-1-2457 (with Jiefang Li, VT)	
Source of Support: Office of Naval Research	Location of Project: Virginia Tech
Award Amount: $326353 Total Award Period Covered: 7/1/2015-9/30/2019	
Award Amount to PI's Research: $326353	
Person-Months Per Year Committed to Project: _0.15___ Pers. Months; Specify: Cal., Acad., or Sumr: Sumr	
Describe Research Including Synergies and Delineation with Respect to this Proposal/Award: Development of magnetic sensors based on magnetoelectric composites that have the ability to reject acoustical/mechanical vibration noise sources. No overlap with present proposal.	

Investigator: Dwight Viehland	Other Agencies to which this proposal has been/will be submitted:
Support (Current, Pending, Submission Planned in Future or Transfer of Support): Current	
Project/Proposal Title and grant number, if appropriate: Reconfigurable Electronics based on Multi-Ferroics and Nano-magnetism (with Jiefang Li, VT) Award number: FA9550-16-1-0001	
Source of Support: AFOSR	Location of Project: Virginia Tech
Award Amount: $434085 Total Award Period Covered: 11/30/2015-10/31-2019	
Award Amount to PI's Research: $434085	
Person-Months Per Year Committed to Project: _0.3___ Pers. Months; Specify: Cal., Acad., or Sumr: Sumr	
Describe Research Including Synergies and Delineation with Respect to this Proposal/Award: Investigation of vertically integrated magnetoelectric nanostructures epitaxially deposited on substrates, and testing of their tunable properties under DC electrical and magnetic biases for applications in next generation electronics. There are some synergies with the DOE program for which this report is written. This synergy concerns property and TEM measurements. It is distinct from this DOE program, as it focused on a wide variety of nanostructures for tunable properties, whereas the DOE project focused on E-field control of $BiFeO_3$. They were also clearly delineated in student thesis, as the AFOSR grant supported Xiao Tang and the DOE grant supported Min Gao.	

Investigator: Dwight Viehland	Other Agencies to which this proposal has been/will be submitted:
Support (Current, Pending, Submission Planned in Future or Transfer of Support): Current	
Project/Proposal Title and grant number, if appropriate: Nano-Domain and Defect Engineering of Binary and Ternary-modified PMN-PT Textured Ceramics and Crystals (with Jiefang Li, VT) Award number: N00014-17-1-2234	
Source of Support: Office of Naval Research	Location of Project: Virginia Tech
Award Amount: $382573 Total Award Period Covered: 3/1/2017- 2/28/2020	
Award Amount to PI's Research: $382573	
Person-Months Per Year Committed to Project: ____ Pers. Months; Specify: Cal., Acad., or Sumr:	
Describe Research Including Synergies and Delineation with Respect to this Proposal/Award: Investigations of nanodomain engineering in single crystals and textured piezoelectric ceramics. Determination of how the phase transformation sequence and domain conditions are effected by such compositional modifications. No overlap with present proposal.	

Investigator: Dwight Viehland	Other Agencies to which this proposal has been/will be submitted:
Support (Current, Pending, Submission Planned in Future or Transfer of Support): Current	
Project/Proposal Title and grant number, if appropriate: Mesoscale interfacial dynamics in magnetoelectric nanocomposites (with Shashank Priya, VT) Award number: DE-FG02-06ER46290	
Source of Support: DOE	Location of Project: Virginia Tech
Award Amount: $1866262 Total Award Period Covered: 8/1/2006-7/31/2018	
Award Amount to PI's Research: $1866262	
Person-Months Per Year Committed to Project: _0.3___ Pers. Months; Specify: Cal., Acad., or Sumr: Sumr	
Describe Research Including Synergies and Delineation with Respect to this Proposal/Award: Deposition and investigation of phase transitions in epitaxially deposited BiFeO3 on PMN-PT substrates. Engineering of magnetic phase transitions through strain engineering. This is the program for which the report was written. There were some synergies with the AFOSR program listed and detailed above. It is distinct from this DOE program, as the AFOSR program focused on a wide variety of nanostructures for tunable properties, whereas the DOE project focused on E-field control of $BiFeO_3$. They were also clearly delineated in student thesis, as the AFOSR grant supported Xiao Tang and the DOE grant supported Min Gao.	

Investigator: Dwight Viehland	Other Agencies to which this proposal has been/will be submitted:
Support (Current, Pending, Submission Planned in Future or Transfer of Support): Current	
Project/Proposal Title and grant number, if appropriate: A MATRIX Solution to Solid State Devices for Scalable, Integratable, and Efficient Signal and Power (with Jiefang Li, VT) Award number: W911NF-15-1-0616	
Source of Support: Army Research Office	Location of Project: Virginia Tech
Award Amount: $1499980 Total Award Period Covered: 10/1/2015-6/30/2019	
Award Amount to PI's Research: $902887	
Person-Months Per Year Committed to Project: __1__ Pers. Months; Specify: Cal., Acad., or Sumr: Sumr	
Describe Research Including Synergies and Delineation with Respect to this Proposal/Award: Development and studies of gyrators based on magnetoelectric heterostructures. Gyrators have a unique ability to convert current into voltage, and offer important features with regards to electrical and magnetic property inversion. No overlap with present proposal.	

Investigator: Dwight Viehland	Other Agencies to which this proposal has been/will be submitted:
Support (Current, Pending, Submission Planned in Future or Transfer of Support): Award in Process	
Project/Proposal Title and grant number, if appropriate: Material Solution for Electron Transpiration Cooling of Leading Edges: E.T.-cooling (with Jiefang Li)	
Source of Support: Defense Advanced Research Projects Agency Location of Project: Virginia Tech	
Award Amount: $1,815,000 Total Award Period Covered: 12/09/19-12/08/23	
Award Amount to PI's Research: $1,815,000	
Person-Months Per Year Committed to Project: __0.15__ Pers. Months; Specify: Cal., Acad., or Sumr: 0.15 Sumr	

8. Cost status: Show approved budget by the budget period, actual costs incurred by the date of the report and projected unspent funds at the end of the current budget period. If any cost-sharing is required, breakout by DOE share, recipient share and total costs.

All Funds expended

References

[1] Shuxiang Dong, Junyi Zhai, Jiefang Li, and D. Viehland, Applied Physics Letters **89** (25), 252904 (2006).

[2] Yaojin Wang, David Gray, David Berry, Junqi Gao, Menghui Li, Jiefang Li, and Dwight Viehland, Advanced Materials **23** (35), 4111 (2011).

[3] B. Hu, Y. Chen, A. Yang, S. Gillete, Trifon Fitchorov, A. Geiler, A. Daigle, X. D. Su, Z. Wang, D. Viehland, C. Vittoria, and V. G Harris, Journal of Applied Physics **111** (7), 07D916 (2012).

[4] Zhiguang Wang, Yanxi Li, Wenwei Ge, Ravindranath Viswan, Jiefang Li, and Dwight Viehland, Materials Letters **113**, 159 (2013).

[5] Haribabu Palneedi, Deepam Maurya, Gi-Yeop Kim, Shashank Priya, Suk-Joong L. Kang, Kwang-Ho Kim, Si-Young Choi, and Jungho Ryu, Applied Physics Letters **107** (1), 012904 (2015).

[6] Haribabu Palneedi, Insung Choi, Gi-Yeop Kim, Venkateswarlu Annapureddy, Deepam Maurya, Shashank Priya, Jong-Woo Kim, Keon Jae Lee, Si-Young Choi, Sung-Yoon Chung, Suk-Joong L. Kang, and Jungho Ryu, Journal of the American Ceramic Society **99** (8), 2680 (2016).

[7] Haribabu Palneedi, Deepam Maurya, Gi-Yeop Kim, Venkateswarlu Annapureddy, Myoung-Sub Noh, Chong-Yun Kang, Jong-Woo Kim, Jong-Jin Choi, Si-Young Choi, Sung-Yoon Chung, Suk-Joong L. Kang, Shashank Priya, and Jungho Ryu, Advanced Materials **29** (10), 1605688 (2017).

[8] M. I. Bichurin, V. M. Petrov, and G. Srinivasan, Physical Review B **68** (5), 054402 (2003).

[9] D. Barrionuevo, N. Ortega, A. Kumar, R. Chatterjee, J. F. Scott, and R. S. Katiyar, Journal of Applied Physics **114** (23), 234103 (2013).

[10] F. Yang, N. Kemik, M. D. Biegalski, H. M. Christen, E. Arenholz, and Y. Takamura, Applied Physics Letters **97** (9) (2010).

[11] J. H. Liao and T. B. Wu, Electrochem Solid St **10** (10), P27 (2007); J. H. Liao, T. B. Wu, Y. T. Chen, and J. M. Wu, Journal of Applied Physics **101** (9) (2007); S. R. Spurgeon, P. V. Balachandran, D. M. Kepaptsoglou, A. R. Damodaran, J. Karthik, S. Nejati, L. Jones, H. Ambaye, V. Lauter, Q. M. Ramasse, K. K. S. Lau, L. W. Martin, J. M. Rondinelli, and M. L. Taheri, Nat Commun **6** (2015).

[12] C. A. F. Vaz, J. Hoffman, Y. Segal, J. W. Reiner, R. D. Grober, Z. Zhang, C. H. Ahn, and F. J. Walker, Phys Rev Lett **104** (12) (2010).

[13] J. D. Burton and E. Y. Tsymbal, Physical Review B **80** (17) (2009); H. J. A. Molegraaf, J. Hoffman, C. A. F. Vaz, S. Gariglio, D. van der Marel, C. H. Ahn, and J. M. Triscone, Advanced Materials **21** (34), 3470 (2009).

[14] E. A. Kraut, R. W. Grant, J. R. Waldrop, and S. P. Kowalczyk, Phys Rev Lett **44** (24), 1620 (1980).

[15] M. Clavel, P. Goley, N. Jain, Y. Zhu, and M. K. Hudait, Ieee J Electron Devi **3** (3), 190 (2015); M. Clavel, D. Saladukha, P. S. Goley, T. J. Ochalski, F. Murphy-Armando, R. J. Bodnar, and M. K. Hudait, Acs Appl Mater Inter **7** (48), 26470 (2015).

[16] C. L. Wu, P. W. Lee, Y. C. Chen, L. Y. Chang, C. H. Chen, C. W. Liang, P. Yu, Q. He, R. Ramesh, and Y. H. Chu, Physical Review B **83** (2) (2011).